

UNCLASSIFIED

AD NUMBER
AD487455
NEW LIMITATION CHANGE
TO Approved for public release, distribution unlimited
FROM Distribution: USGO: others to Director, Defense Atomic Support Agency, Washington, D. C. 20301.
AUTHORITY
DTRA ltr, 3 Nov 99

THIS PAGE IS UNCLASSIFIED

7
48
DASA-1801

IITRI

BEHAVIOR OF EXPLOSIVE SYSTEMS
UNDER MILD IMPACT

by

H. S. Napadensky

and

J. E. Kennedy

May 1966

Each transmittal of this document outside
the agencies of the U. S. Government must
have prior approval of the Director, Defense
Atomic Support Agency, Washington, D. C.

BLANK PAGE

DASA-1801

IIT RESEARCH INSTITUTE
10 West 35 Street
Chicago, Illinois 60616

IITRI Project T6111
Contract DA-49-146-XZ-374

BEHAVIOR OF EXPLOSIVE SYSTEMS
UNDER MILD IMPACT

Final Report

by

H.S. Napadensky
and
J.E. Kennedy

for

Director, Defense Atomic Support Agency
Washington, D. C.

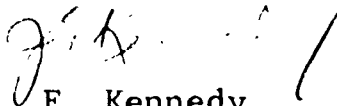
May 31, 1966

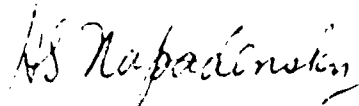
FOREWORD

This final report on IITRI Project T6111, "Behavior of Explosive Systems under Mild Impact," describes studies carried out for the Defense Atomic Support Agency under Contract DA-49-146-XZ-374 during the period 1 November 1964 to 30 April 1966.

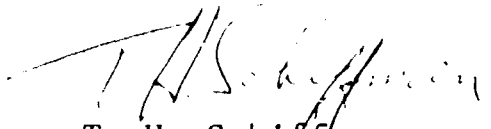
Personnel who have contributed to the work discussed in this report include: D. Baker, R. H. Blumenthal, J. Daley, C. Groom, H. Karplus, J. E. Kennedy, H. S. Napadensky (Project Engineer), and M. Surdel.

Respectfully submitted,
IIT Research Institute


J. E. Kennedy
Research Engineer


H. S. Napadensky
Research Engineer and
Group Leader

APPROVED:


T. H. Schiffman
Assistant Director
Geophysics Research

ABSTRACT

Analytical and experimental studies were carried out to increase the understanding of the behavior of high explosives under impact loads. A mathematical model of the impact initiation phenomena was constructed assuming that a single mechanism, viscous heating, was operating during the radial extrusion of a flat explosive billet. Techniques were developed for continuously monitoring the temperature profile at the explosive-anvil interface, using rapid response (1.5μ sec) surface thermocouples to check the adequacy of the analytical model. The results of these experiments showed that the highest temperatures were obtained at the outer edge along the HE-anvil interface as predicted by the viscous heating model.

To extend the applicability of the IITRI-developed method for predicting impact velocities required for the initiation of the explosive components of special weapons, basic sensitivity data was acquired for 9010 PBX, Comp B-3 and 9404 PBX. In particular, the explosives were subjected to a concentrated impact load by means of a wedge shaped loading device and to planar uniform loads having two different pulse shapes. Analyses of the wave propagation in layered segments consisting of inert and explosive materials were carried out to predict the impact velocity required to initiate the explosive in such a system. Impact experiments on these models confirmed the validity of the prediction method.

BLANK PAGE

TABLE OF CONTENTS

	<u>Page</u>
FOREWORD	ii
ABSTRACT	iii
LIST OF FIGURES	vii
LIST OF TABLES	viii
I. INTRODUCTION	1
II. MECHANISM OF INITIATION BY LOW-VELOCITY IMPACT	4
A. Summary of This Mechanism Study	7
B. Impact Extrusion Analysis	9
C. Experiments with Rapid Response Thermocouples	14
1. Thermocouple Response Time Measurements	16
2. Instrumented Impact Extrusion Experiments	20
3. Operational Notes	28
III. STUDIES TO EXTEND THE APPLICABILITY OF PREDICTING THE VULNERABILITY OF WEAPONS TO IMPACT	29
A. Experimental Procedures	29
1. The Explosive Materials	29
2. Experimental Arrangement	31
3. Criteria of Fire	32
4. Velocity of Sound Measurements	33
5. Driver Plate Velocities	36
B. Results of Experiments	36
1. Planar Impact Loading	36
2. Concentrated Impact Loading	47
3. Sensitivity of Detonators	51
4. Velocity of Sound in 9010 PBX	53
5. One-Dimensional Composites, Analysis And Experiments	54

TABLE OF CONTENTS (Continued)

	<u>Page</u>
IV. CONCLUSIONS AND RECOMMENDATIONS	59
APPENDIX	61
REFERENCES	65
Distribution List	67
DDC Form 1473	73

LIST OF FIGURES

<u>Figure</u>	<u>Page</u>
1. Critical impact velocity as a function of explosive length, for 6-in.-diameter 9404 PBX billets impacted by 6-in.-diameter by 1-in.-thick steel plates	2
2. Test arrangement	5
3. Model for calculation of viscous heating due to radial impact extrusion	10
4. Rapid response Nanmac surface thermocouple	15
5. Surface thermocouple positions on anvil	17
6. Oscilloscope records of thermocouple response time measurements	19
7. Response time as a function of thermocouple resistance	21
8. Circuit diagram and calibration records for intermittent monitoring of thermocouple resistance histories	23
9. Oscilloscope records of impact extrusion experiments	27
10. Configurations for planar impact experiments prior to acceleration of driver plate	37
11. Results of planar impact experiments, various lengths of explosives	40
12. Wedge-shaped impact loading device	48
13. One-dimensional composites which were used as models for wave propagation calculations and impact experiments to validate prediction technique	55
14. Computed particle velocity at the explosive, for layered composites detailed in Figure 13	56
15. Graphic method for obtaining (P, U_p) at the interface of two materials upon impact	64

LIST OF TABLES

<u>Table</u>		<u>Page</u>
I	Results of Impact Experiments Instrumented With Surface Thermocouples	26
II	Summary of Planar Impact Experiments	41
III	Summary of Wedge Impact Experiments	49
IV	Impact Experiments on Detonators	52
V	Sound Velocity and Elastic Constants of 9010 PBX	53
VI	Summary of Experiments on Layered Materials	58

BEHAVIOR OF EXPLOSIVE SYSTEMS UNDER MILD IMPACT

I. INTRODUCTION

Within recent years IITRI has conducted studies directed toward developing a method for predicting the response of weapons to a wide variety of severe impact conditions. Laboratory studies carried out in pursuit of this problem established some of the important parameters governing the impact initiation of large charges of high explosives. Two noteworthy observations have been made through these experiments. First, impact velocity, rather than impact energy or momentum, has been found to govern the response of the explosive. Secondly, the impact velocity required for initiation is strongly dependent on charge size (Ref. 1), as Figure 1 shows. The experimentally obtained data on the impact sensitiveness of explosives coupled with an analytical method that takes into account the effect of the particular weapon configuration have formed the basis for enabling us to achieve the goal of predicting the impact vulnerability of weapons (Ref. 1,2,3). The predicted values have been in good agreement with the results of field tests in a large majority of cases (Ref. 4).

Although the original goal of developing a method for predicting the impact response of weapons had been achieved, impact experiments on large charges of explosives are still required to determine the response of new explosive formulations. Data obtained by means of the standard small scale impact drop tests (Ref. 5) (on explosives of the order of grams in weight) cannot be quantitatively extrapolated to determine the response of large charges (Ref. 6). Further, detonation of large charges of explosives can occur at impact speeds and pressures that are well below those predicted by one-dimensional shock theory (Ref. 7,8). Part of the inability to either extrapolate from very small charge data to predictions of the response of large charges or

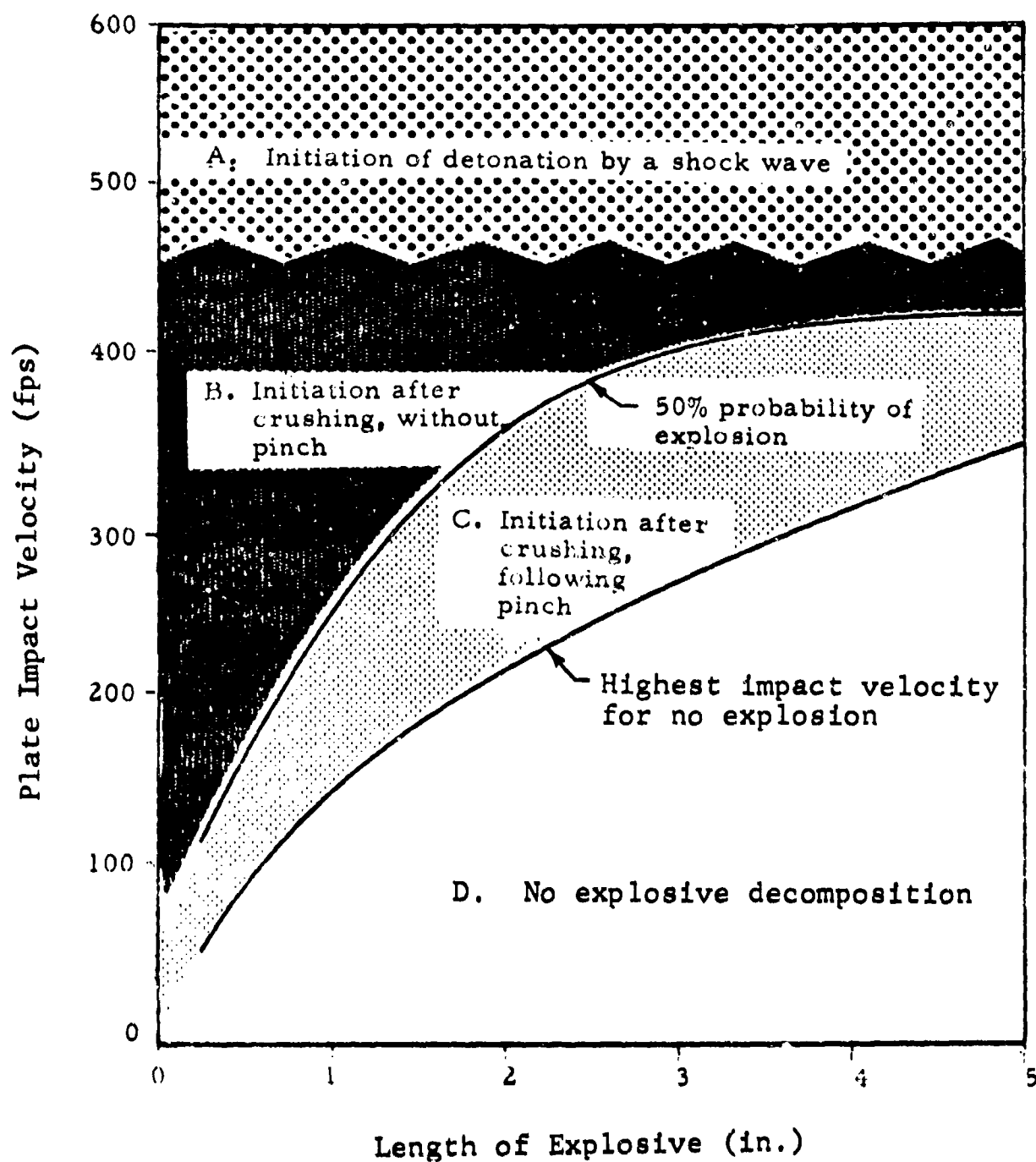


Figure 1 Critical impact velocity as a function of explosive length, for 6-in.-diameter 9404 PBX billets impacted by 6-in.-diameter by 1-in.-thick steel plates

to predict response from shock theory is due to a lack of understanding of the various mechanisms by which explosives react when they are subjected to gentle impact.

Hence, one of the objects of the work reported here was to conduct both analytical and experimental studies directed toward gaining an understanding of the mechanisms responsible for initiation at low impact velocities. Analytical studies can reveal parameters whose role or significance is masked in interpretations of experimental results. Insight into hazardous conditions not tested in the laboratory may also be revealed by an analytical model. A knowledge of mechanisms governing the initiation process can provide guidelines for the formulation of new explosives or modification of existing explosives that will reduce their impact sensitivities. Moreover, a knowledge of the mechanisms controlling the impact response of high explosives would reduce the amount of testing required to determine the sensitivity of a new explosive material.

The other objective of the work reported here was to extend the applicability of the method for predicting vulnerable impact velocities for weapons by acquiring additional sensitivity data. Further, experiments were conducted on layered segments containing inert and explosive materials to simulate weapon configurations for the purpose of confirming the validity of the prediction method.

The experimental technique that was used to determine the impact sensitiveness of high explosives was intended to simulate, under laboratory conditions, configurations which would exist in a weapon, i.e., with the explosive confined on two sides by high-impedance materials. The experimental setup was simple enough that data obtained regarding the physical quantities involved in characterizing the impact phenomena permitted interpretations to different weapon configurations. Basically, in each experiment a laterally unconfined explosive billet was impacted between a moving steel plate (driver plate) and a stationary steel anvil, Figure 2.

11. MECHANISM OF INITIATION BY LOW-VELOCITY IMPACT

High-speed framing camera photographs have shown the crushing and subsequent initiation processes in impacted explosive billets (Ref. 1). The regions denoted as A, B, C, and D in Figure 1 exhibited differences in behavior that carry implications regarding the mechanism of initiation in the respective regions. While Figure 1 pertains specifically to 9404 PBX, other explosives such as H-6 (Ref. 3) and Tritonal (Ref. 9) exhibited generally similar behavior but with higher velocities required for initiation of these less sensitive explosives.

In region A of Figure 1, high-order detonations occur at impact velocities above 440 fps and calculated pressures of the order of 10 kilobars. Explosions occur within the first 10 to 100 μ sec after impact, during the first passage of the nonreactive stress wave through the explosive billet or immediately upon reflection of this stress pulse from the back-up anvil.

In region B, initiation of explosion occurs at impact velocities less than 440 fps and after some small amount of crushing and lateral extrusion of the explosive billet occurs. The explosion which may be a violent deflagration or detonation of part of the explosive still trapped between the driving plate and the anvil occurs within 100 msec to 1 sec after impact.

In region C, which we consider to be the initiation threshold region, explosions occur only after the majority of the explosive has been extruded beyond the original diameter and the remaining explosive is crushed to a very thin layer. This "pinch" condition has been observed to occur within 1 to 3 msec after impact for the plastic bonded HMX-based materials (Ref. 2). Under these loading conditions the explosive is entirely consumed in a mild reaction.

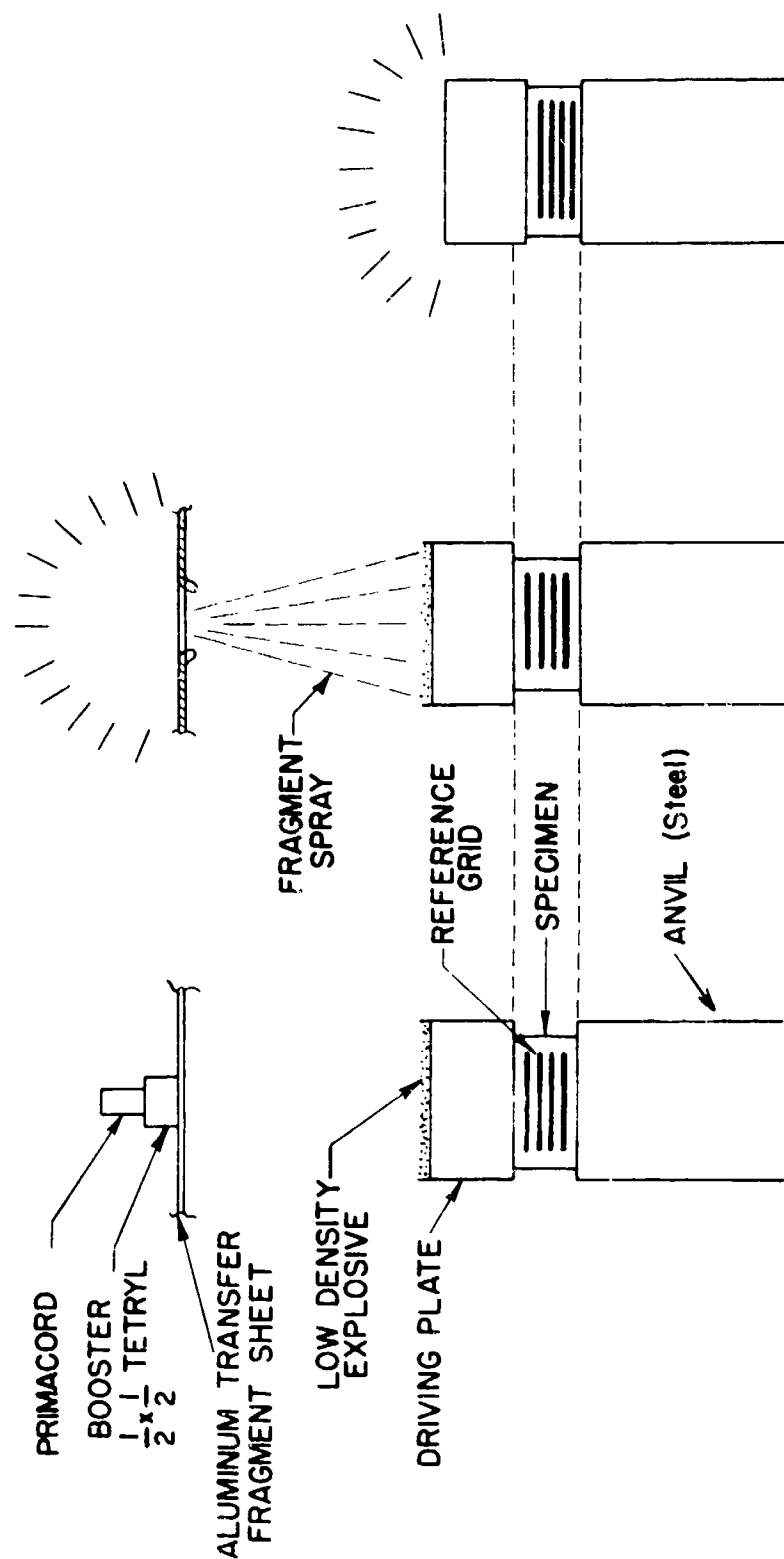


Figure 2 Test arrangement

Explosions do not occur in region D, the no-go region. Under these conditions a layer of unreacted explosive remains on the witness plate after impact.

Finally, we observe explosions occurring external to the original charge diameters and after complete crushup and extrusion of the billet. Here the explosion originates in the explosive dust which was extruded from between the colliding plates. This type of reaction can cause considerable damage and noise.

Region C, wherein marginal initiation can occur at minimal impact velocities, is of greatest interest in considering the impact hazard of explosive systems. The marginal ignition of unconfined solid high explosives by low-velocity impact is unlike shock initiation in a number of important respects. Reaction can be initiated within the first several microseconds in shock initiation experiments, or a propagating reaction will not be initiated at all; in contrast, the low-velocity impact process as in region C may continue for a few milliseconds before ignition is observed. During this long pre-ignition period, there is substantial crushing of the explosive charge, and crushed material is ejected radially at rather high velocities. The input shock pressures induced in the explosive by low-velocity impact at marginal ignition conditions, perhaps as low as 1 to 6 kilobar (Ref. 10, 11, 12), are an order of magnitude lower than those required to cause shock initiation (Ref. 7, 8). The long time delay to ignition under low-velocity impact permits hundreds of reflections of compressive stress waves in the explosive between the high impedance driving plate and anvil. In elastic materials, such multiple reflections cause increases in the stress level, but because solid explosives attenuate unreactive acoustic or stress waves drastically (Ref. 2), there is a question as to whether the net stress level in the explosive would increase above a few kilobars, or decrease with time during the impact process.

Because of these gross dissimilarities in the behavior of explosives experiencing shock initiation at shock velocities of 20 ft/sec or more as opposed to initiation under "gentle" low-velocity impact, it is reasonable to believe that localized heating, leading to ignition of the explosive, may be brought about by processes other than shock heating. Bowden and Yoffe (Ref. 13), for instance, have shown that initiation of small explosive samples by the impact of weights dropped from height of 1 to 80 cm is achieved by a mechanism of adiabatic heating of occluded gas bubbles. Bowden has suggested a number of processes as possible mechanisms of ignition, which are best presented as a direct quotation from Reference 14: "Initiation may be brought about in the following ways

- (1) "by heat which raises the material to the ignition temperature,
- (2) "by impact or shock, this can act by:
 - (a) an adiabatic heating of compressed gas spaces,
 - (b) a frictional hot spot on the confining surface or on a grit particle,
 - (c) intercrystalline friction of the explosive itself;
 - (d) viscous heating of the explosive at high rates of shear,
 - (e) heating of a sharp point when it is deformed plastically,
 - (f) mutual reinforcement of gentle shock waves,
- (3) "by ultrasonic vibration,
- (4) "by electrons, α particles, neutrons, and fission fragments,
- (5) "by light of sufficient intensity,
- (6) "by electric discharge,
- (7) "by spontaneous initiation of a growing crystal.

A Summary of This Mechanism Study

Because of the high radial velocity imparted to the crushed explosive particles in our low velocity driving plate impact experiments, it was believed that the viscous heating mechanism

might apply to our experimental configuration. A mathematical model of the impact process was developed to determine whether viscous flow processes appeared to be capable of converting a sufficient amount of mechanical energy into localized heating to cause ignition of the explosive.

A preliminary analysis indicated that ignition due to local viscous heating indeed appeared possible. It was found that knowledge of the value of the coefficient of viscosity of the explosive under the calculated local conditions of temperature, pressure, and rate of strain was needed to make further progress quantitatively on the mathematical model. Such viscosity data do not exist, and can only be generated by making experimental measurements of this property.

Before devoting further effort to analysis or embarking on an experimental program to measure the coefficient of viscosity of solid explosive under high rates of strain, an attempt was made to experimentally determine whether certain qualitative conclusions drawn from the preliminary analysis were in fact valid. The analysis had indicated that viscous heating would cause the greatest local temperature rise adjacent to the surface of the anvil, at a radial position near the periphery of the driving plate. An independent analysis by Weston (Ref. 15) indicated the same conclusion regarding the position of greatest temperature rise, assuming a model in which the dominant mechanism of conversion of mechanical energy to heat was friction at the interface between the explosive and the anvil.

Fast-response surface thermocouples were obtained and were embedded in the anvil at the center, halfway to the outer (driving plate) radius, and just inside the outer radius. The results of several experiments using 90010 mock explosive and 9404 PBX appeared to confirm that very significant heating occurs at the interface apparently due to flow processes during impact, since the variation in temperature rise as a function of position agreed qualitatively with the flow models.

This work thus suggests that lateral flow processes may be responsible for ignition of solid explosives under low-velocity impact.

The following sections describe the analytical and experimental investigation of the viscous heating model for the impact ignition of solid explosives.

B. Impact Extrusion Analysis

The impact of a steel driving plate upon a large cylindrical explosive billet causes radial extrusion of the explosive. In beginning to analyze such a flow we must first determine the flow regime, i.e., whether laminar or turbulent. Reynolds numbers, Re , were calculated for quite severe loading conditions, assuming the viscosity of the explosive to be 10^6 poise (Ref. 16) and using the height between the driving plate and anvil as the "characteristics length." An equation expressing conservation of mass in the extrusion flow indicates that mass flow rate is highest at the outer periphery of the driving plate ($r = R_p$) at any given time.

Let us define the following terms, to which we refer in Figure 3 and subsequent equations

- r = radial position (variable) about axis of cylindrical charge
- h = axial position (variable) Datum plane is at anvil surface
- H = axial distance between the anvil and driving plate surface at any given time. $H = H(t)$.
- u = radial velocity. $u = u(r, h)$
- \bar{u} = average radial velocity at a given radial position, $\bar{u} = \bar{u}(r, t)$
- \bar{G} = average mass flow rate at a given radial position, mass per unit time per unit area, $\bar{G} = \bar{G}(r)$
- ρ = density of explosive (assumed constant)
- μ = viscosity of explosive (assumed constant)
- v_p = driving plate impact velocity (assumed constant)

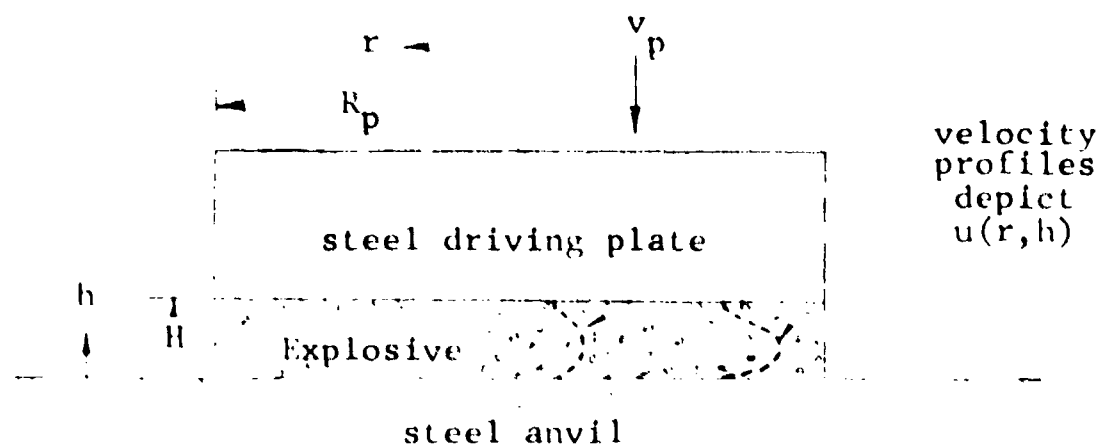


Figure 3 Model for calculation of viscous heating due to radial impact extrusion.

and $G(r) = \bar{u}_r = \frac{v_p r}{2H}$ (from a mass balance),

$$Re(r) = \frac{HG(r)}{\mu} = \frac{v_p r}{2\mu} \quad (1)$$

It is significant to note that Reynolds number is independent of H . To find a maximum Reynolds number, we consider a maximum plate velocity of 1000 fps and maximum radius, $R_p = 3\text{in.}$, which generates $Re_{\text{max}} = 0.2$. This value indicates that the extrusion flow must be laminar. All analysis was based on this assumption.

In order to calculate the extent of local dissipation of mechanical energy as viscous heating within the flowing explosive, the velocity profile must be determined. Neglecting inertial effects associated with the velocity of the driving plate, we may show that the velocity profile is parabolic, varying in amplitude as a function of r and H . The driving plate velocity causes a sigmoidal variation in the profile near the driving plate surface (Ref. 17), as sketched in Figure 3. The material near the anvil surface does not possess a significant axial velocity component, so its velocity profile closely follows that derived neglecting inertial effects.

Subsequent analysis will show that the amount of energy locally dissipated into heat by the viscous flow process is a function of the velocity gradient. Since the maximum velocity gradient associated with a parabolic flow profile (as near the anvil) is higher than that associated with the sigmoidal profile (as near the driving plate), it may be concluded that the more pronounced viscous heating will occur near the anvil interface. Furthermore, for preliminary analysis our attention may be directed solely to the parabolic flow profile, neglecting inertial effects, since these effects which are concentrated near the opposite face of the explosive will have very small influence on the velocity profile near the anvil.

Let us write a differential force balance on an annular element of explosive of height dh and width dr , for derivation of the viscous flow velocity profile, equating pressure forces and shear forces. Assume that the solid explosive behaves as a Newtonian fluid of constant viscosity.

$$g_c \left(\frac{dp}{dr} \right) dr \cdot 2\pi r dh = \frac{\eta}{h} \left(\frac{du}{dh} \right) dh \cdot 2\pi r dr \quad (2)$$

Since $\frac{dp}{dr}$ is independent of h , we may integrate twice and apply the boundary conditions (1) at $h = H/2$, $\frac{du}{dh} = 0$ and (2) at $h = 0$, $u = 0$, to derive the flow profile expression

$$u = \frac{g_c}{2\eta} \frac{dp}{dr} (h^2 - hH) \quad (3)$$

We may eliminate $\frac{dp}{dr}$, which is not easily evaluated, from the velocity profile expression by evaluating \bar{u} from Eq. (3) by integration, then equate this to the expression for \bar{u} obtained by a mass balance:

$$\bar{u} = \frac{\int_0^H u \cdot 2\pi r dh}{\int_0^H 2\pi r dh}$$

$$\bar{u} = - \frac{g_c H^2}{12\eta} \frac{dp}{dr}$$

Since $\bar{u} = v_p r / 2H$ from a mass balance,

$$\frac{dP}{dr} = - \frac{6 v_p r}{g_c H^3}$$

Substitute this expression for $\frac{dP}{dr}$ into Eq. (3).

$$u = \frac{3 v_p r (hH - h^2)}{H^3} \quad (4)$$

Note that this expression satisfies all boundary conditions

imposed on $u(r, h)$, i.e., (1) $u(r, 0) = 0$, (2) $u(r, H) = 0$,

(3) $\frac{\partial u}{\partial h} (r, \frac{H}{2}) = 0$, and (4) $u(0, h) = 0$.

Now let us utilize this expression for the velocity profile in the calculation of viscous heating accompanying impact extrusion. The equation of mechanical energy (Ref. 18)

$$\rho \frac{D}{Dt} (u^2/2) = - (\bar{u} \cdot \nabla P) - [\bar{u} \cdot (\nabla \cdot \tau)] + \rho (\bar{u} \cdot \bar{g}) \quad (5)$$

describes the rate of change of kinetic energy per unit mass ($u^2/2$) into potential energy, acceleration, and dissipation into heat. For a Newtonian fluid in a flow wherein all velocity components vanish except the cylindrical radial velocity component $u = u(r, h)$, the rate of dissipation of mechanical energy into heat per unit volume is

$$\dot{\phi}_V = 2\mu \left[\left(\frac{\partial u}{\partial r} \right)^2 + \left(\frac{u}{r} \right)^2 \right] + u \left(\frac{\partial u}{\partial h} \right)^2 - \frac{2}{3} u \left[\frac{1}{r} \frac{\partial}{\partial r} (ru) \right]^2 \quad (6)$$

When the velocity profile of Eq. (4) is entered into Eq. (6), the local rate of heat evolution per unit volume due to viscous flow may be expressed as a function of radial and axial position, instantaneous distance H between the driving plate and the anvil, and driving plate impact velocity v_p .

$$\dot{\phi}_V = \frac{\mu v_p^2}{H^6} \left[12(h^2 H^2 - 2h^3 H + h^4) + 9r^2(H^2 - 4hH + 4h^2) \right] \quad (7)$$

It may be seen by inspection that the maximum $\dot{\phi}_V$ occurs at $r = R_p$ and $h = 0$.

$$\dot{Q}_v \max = \frac{9\mu R_p^2 v_p^2}{H^4} \quad (8)$$

Let us now assume representative values of the quantities u , R_p , v_p , and H to determine the order of magnitude of dissipative heat release. Assume

$$R_p = 3 \text{ in.} = 0.25 \text{ ft} ; H = 0.12 \text{ in.} = 0.01 \text{ ft} \\ (\text{thin wafer, as in "pinch" condition})$$

$$v_p = 50 \text{ fps} ; \mu = 10^6 \text{ poise (Ref. 8).}$$

Then $\dot{Q}_v \max$ equals $14.06 \times 10^{18} \text{ gm/cm sec}^3$.

For an explosive with a density of 1.7 gm/cc and a specific heat of $0.3 \text{ gm-cal/gm}^\circ\text{C}$, the calculated rate of temperature rise under these impact conditions is $450^\circ\text{C}/\mu\text{sec}$ for the explosive adjacent to the anvil interface.

The tremendous rate of local temperature rise indicated by these calculations may not be realized in actual experiments for a number of reasons. The proximity of the massive steel anvil will act as a heat sink to conduct away a large fraction of the evolved heat, estimated by Weston (Ref. 15) as 15/16 the total heat liberation. Perhaps more significantly, the value of viscosity used was estimated as that pertaining to a plastic bonded explosive at room temperature, and shear stress was assumed to obey the laws defining Newtonian fluids; it is expected that the value of effective viscosity would change greatly (perhaps by orders of magnitude) as the explosive's temperature was rapidly raised, that the viscosity may be highly dependent on rate of strain as in many viscoelastic media, and that under dynamic loading the explosive may otherwise behave very differently from a Newtonian fluid.

Despite the gross assumptions that have been necessary, these calculations demonstrate the possible importance of flow phenomena as a mechanism for localized heating to the point of ignition of impacted solid explosives. Even a local temperature rise of perhaps 10°C per microsecond (corrected for heat

loss into the anvil), rather than the much larger value indicated by the preliminary calculations, would be sufficient to lead to ignition within 30 to 50 μ sec.

Because further meaningful analysis along these lines was stymied until realistic data concerning effective viscosity was available, an experimental approach was attempted in order to determine whether the major qualitative points indicated by the theoretical calculations could be experimentally observed.

C. Experiments with Rapid Response Thermocouples

Flow analyses based on two extreme assumptions regarding the rheologic nature of solid explosive material have been carried out. The two assumptions, i.e., that the explosive flows as a Newtonian fluid (see Section II.B) and alternatively that the explosive deforms in slug flow under impact (Ref. 15), both indicated the same qualitative result regarding the location in the explosive which would be heated most due to flow processes. Because the velocity of the extruding explosive is highest near the outer periphery of the material beneath the driving plate, and the velocity gradient is steepest near the interface between the explosive and the anvil, mechanical energy should be deposited as heat in the explosive at the highest rate near the outer periphery of the charge, near the anvil interface.

An experiment was devised to permit us to measure the magnitude of the temperature rise in the explosive at the interface at various radial positions. The sensing elements were rapid response surface thermocouples* of a design shown in Figure 4. Ribbon elements of chromel and alumel, each 0.002 inch thick by about 1/16 inch wide, separated by a mica film 0.0002 inch thick and insulated from the stainless steel thermocouple body by mica film, travel the length of the probe to the sensing tip. On the surface of the probe tip a very thin conductive junction formed between the ribbon elements in

*Manufactured by the Nanmac Corporation, Needham Heights, Mass.

the thermocouple. The junction may be made by mechanical abrasion of the probe tip by emery cloth (the metal burrs which are thus bridged across the mica insulator comprising the junction) or by chemical or vapor deposition of a thin metallic film on the probe tip.

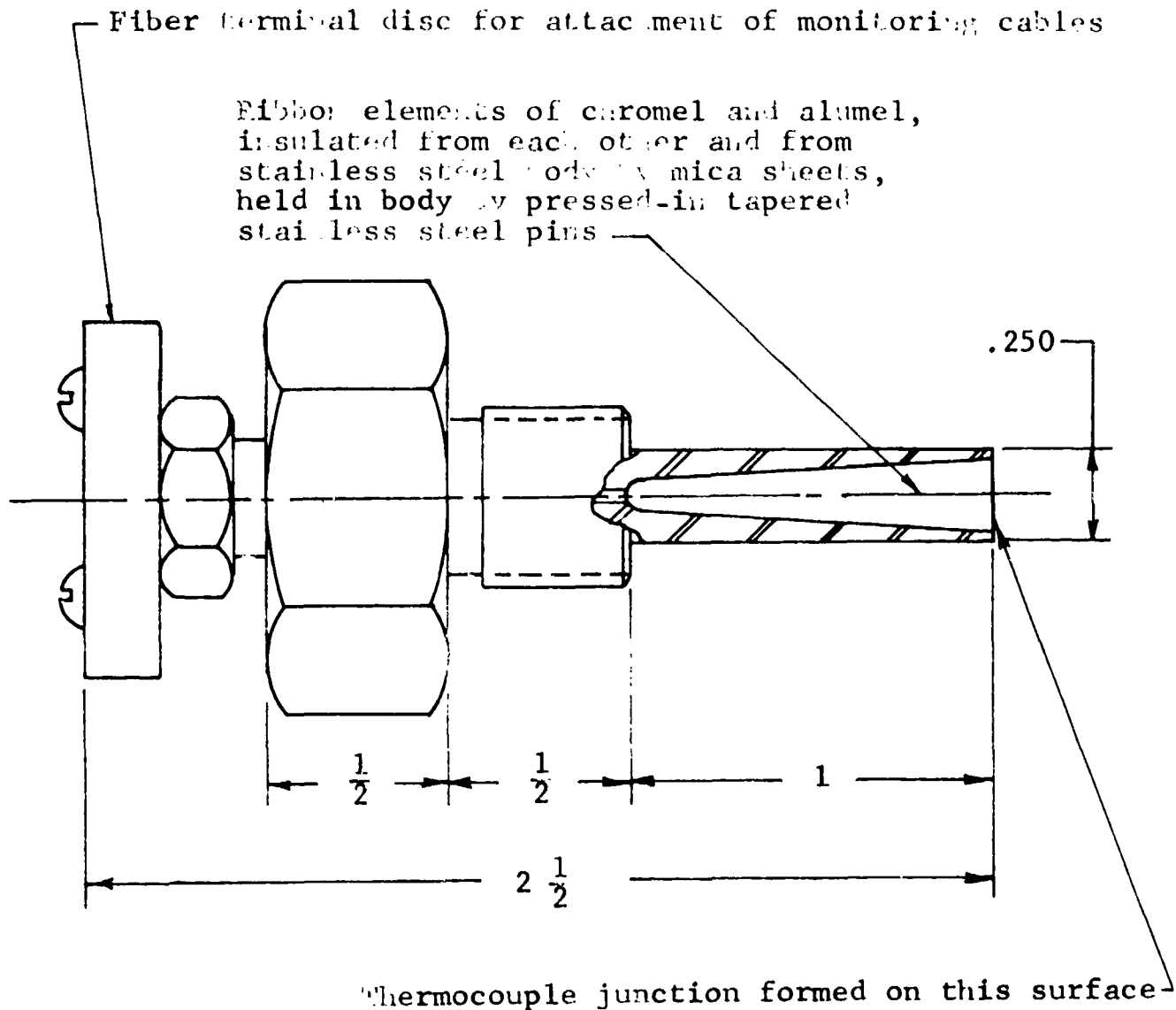


Figure 4 Rapid response Naamac surface thermocouple

The response time of the thermocouple is controlled by the thickness and thermal diffusivity of the conductive material which forms the junction. If a very thin metallic junction (less than one micron thick) can be obtained, the response time is on the order of one microsecond. Marginal initiation in the driving plate impact experiments reported here may occur as late as 1 to 2 milliseconds after impact has begun, so it appeared that microsecond response times would be entirely adequate for observing the temperature history leading toward ignition of high explosives at the anvil interface in impact experiments.

Five surface thermocouples were installed in massive steel anvil plates to permit monitoring of surface temperature histories at three different radial positions, as sketched in Figure 5. A single thermocouple was mounted at the center ($r/R_p = 0$), and two thermocouples were mounted at each of two other radial positions, at $r/R_p = 0.46$ and at $r/R_p = 0.92$ (just inside the outer driving plate periphery). The surfaces of the thermocouples were carefully aligned with the surface of the anvil. The object of experiments with these instrumented anvils was to determine whether experimental observations would bear out the analytical indication that temperature rises should be higher at larger radial positions, and whether the magnitude of the maximum observed temperature rise approached values required to cause cookoff in solid high explosives.

After experiments were conducted to measure the response times of thermocouples with junctions prepared in various ways, impact experiments were performed with 90010 plastic bonded mock explosive and with PBX 9404 samples with instrumented anvils.

1. Thermocouple Response Time Measurements

According to manufacturer's information (Ref. 19) the response time of Nanmac surface thermocouples decreases from about 1 millisecond when the resistance of the thermocouple

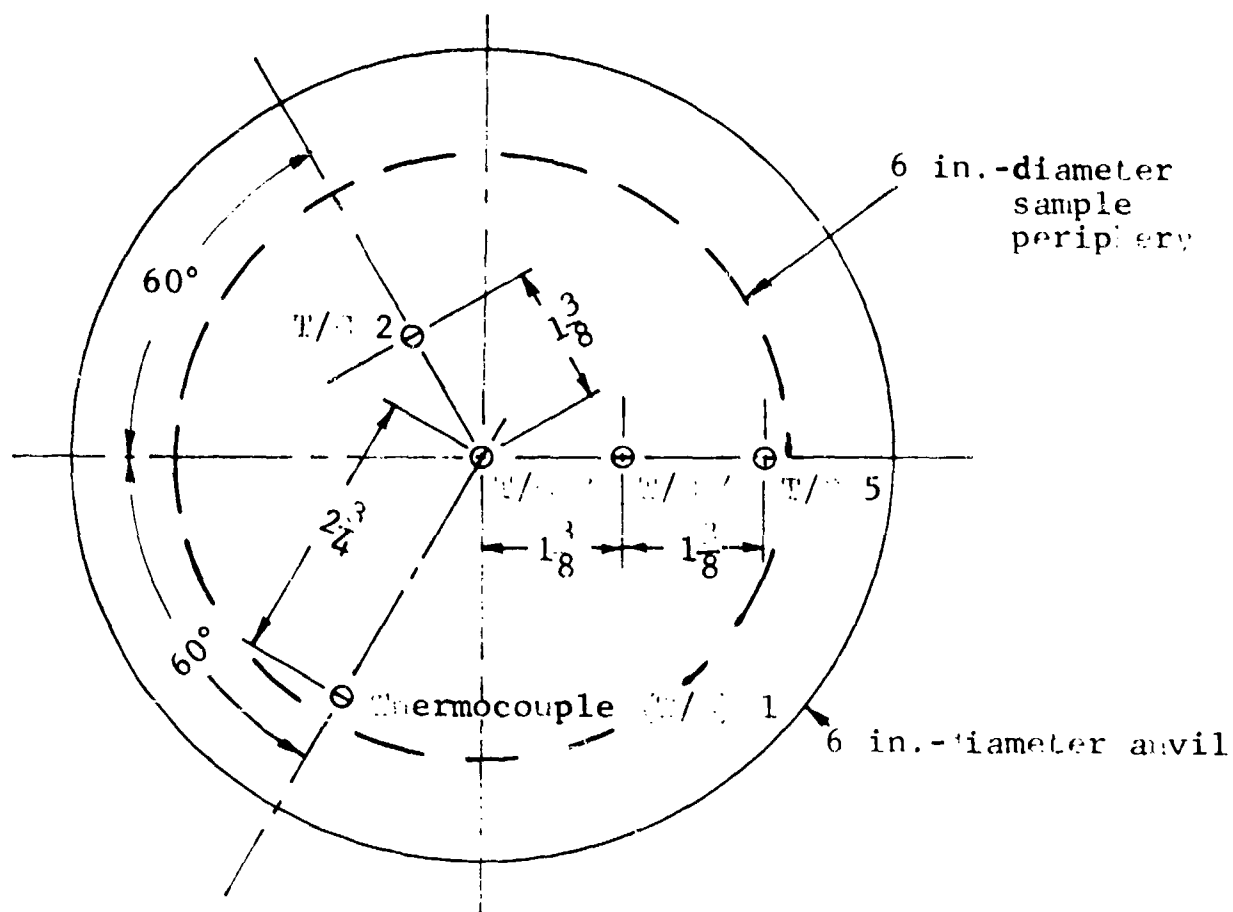


Figure 5 Surface thermocouple positions on anvil

Note: Anvil is 3-in.-thick mild steel. Thermocouples are threaded into appropriate machined cavities in bottom face, to be flush with anvil surface.

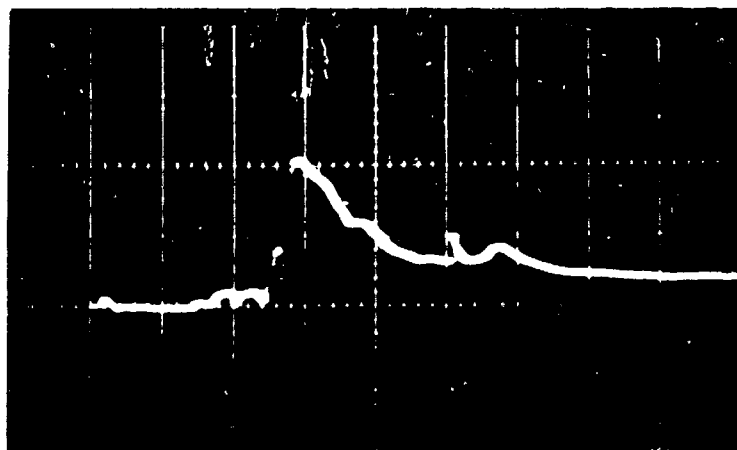
(with mechanically abraded junction) is about 2 ohms, down to about 10 microseconds when the resistance is about 15 ohms. Careful workmanship is necessary to produce a thermocouple junction with a resistance of 15 ohms or higher.

Thermocouple junctions were also produced by vapor deposition of a thin chromium film (estimated to be on the order of 100 angstroms thick) on the surface of the probe tip. Chromium was chosen over other metals because its hardness was expected to reduce wear and abrasion of the film during the impact extrusion of the relatively coarse-grained explosive material.

Junctions of various resistances formed by mechanical abrasion and by vapor deposition were subjected to response time experiments to determine the effect of these variables on response time. The junction was exposed to a sharp-fronted temperature pulse with an exponentially decaying tail, and response time was represented as the time to the maximum thermocouple output. In early experiments, the sudden temperature pulse was produced electrically in some way such as the explosion of a wire by a high current pulse, but the electrical noise associated with the stimulating pulse masked the output signal from the thermocouple, which was less than 10 millivolts.

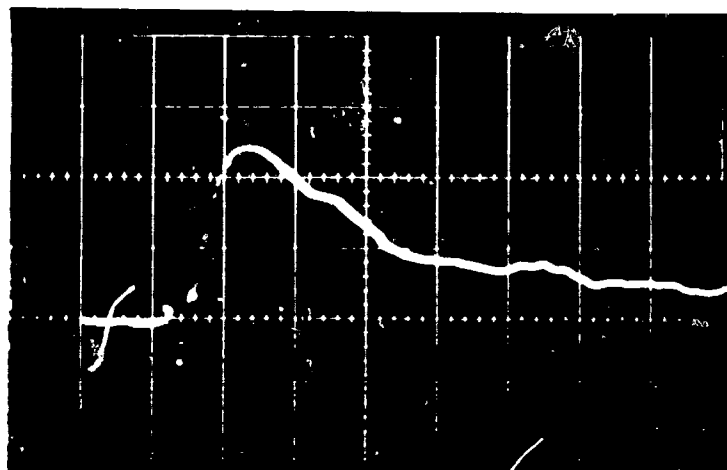
To preclude this problem, the input temperature pulse was generated chemically, by the detonation of a blasting cap. The blasting cap was placed on a heavy steel plate within 1/4 inch of the end of the plate. The thermocouple was positioned "around the corner" of the plate and mechanically decoupled from the plate, such that the entire thermocouple was protected from direct blast but the shock wave turning the corner of the plate would impinge directly on the sensing probe tip. This method produced quite clear oscilloscope traces of thermocouple emf output as a function of time, from which response times were estimated, as shown in Figure 6.

Response times of five microseconds or less were found to be attainable with vapor deposited junctions and with



—→ t

- (a) Vertical scale: 2 mv/cm, corresponds to $\sim 50^{\circ}\text{C}/\text{cm}$
 Horizontal scale: 5 $\mu\text{sec}/\text{cm}$.
 Thermocouple resistance = 12Ω
 Indicated rise time is $\sim 5 \mu\text{sec}$



—→ t

- (b) Vertical scale: 2 mv/cm, corresponds to $\sim 50^{\circ}\text{C}/\text{cm}$
 Horizontal scale: 5 $\mu\text{sec}/\text{cm}$.
 Thermocouple resistance = 20Ω
 Indicated rise time is $\sim 2 \mu\text{sec}$

Figure 6 Oscilloscope records of thermocouple response time measurements.

mechanically abraded junctions of resistance greater than 10 ohms, as illustrated in Figure 7. As a means of checking the veracity of these rapid response signals, experiments were run in which the junction was intentionally covered with a thin layer of oil or shielded in some way from the heat pulse; these experiments showed the anticipated degradation in thermocouple response, which tended to verify the credibility of the direct measurements of response time.

The results of these response time experiments indicated that mechanically abraded junctions exhibited response time just as short as vapor-deposited junctions of minimal metal thickness, and that junctions of either type responded rapidly enough to be satisfactory for monitoring impact extrusion experiments.

The vapor deposited junctions sometimes showed fluctuations in resistance or loss of continuity apparently due to oxidation after a few days of exposure to air.

At this point mechanical abrasion appeared to be superior to vapor deposition as a method for making junctions because junctions could thus be made very economically at the field laboratory site of the explosive experiments, without specialized equipment. Nevertheless, both types of junctions continued to be considered for instrumented impact extrusion experiments with explosives because it was not known whether the flowing explosive would seriously abrade the junctions, and which type of junction could best resist such abrasion.

2. Instrumented Impact Extrusion Experiments

In choosing test conditions for the first impact tests with anvils instrumented with surface thermocouples, it was decided that thin explosive samples would be used because the sensitive "pinch" condition is reached at an earlier time and under a lower plate velocity than required for thicker explosive

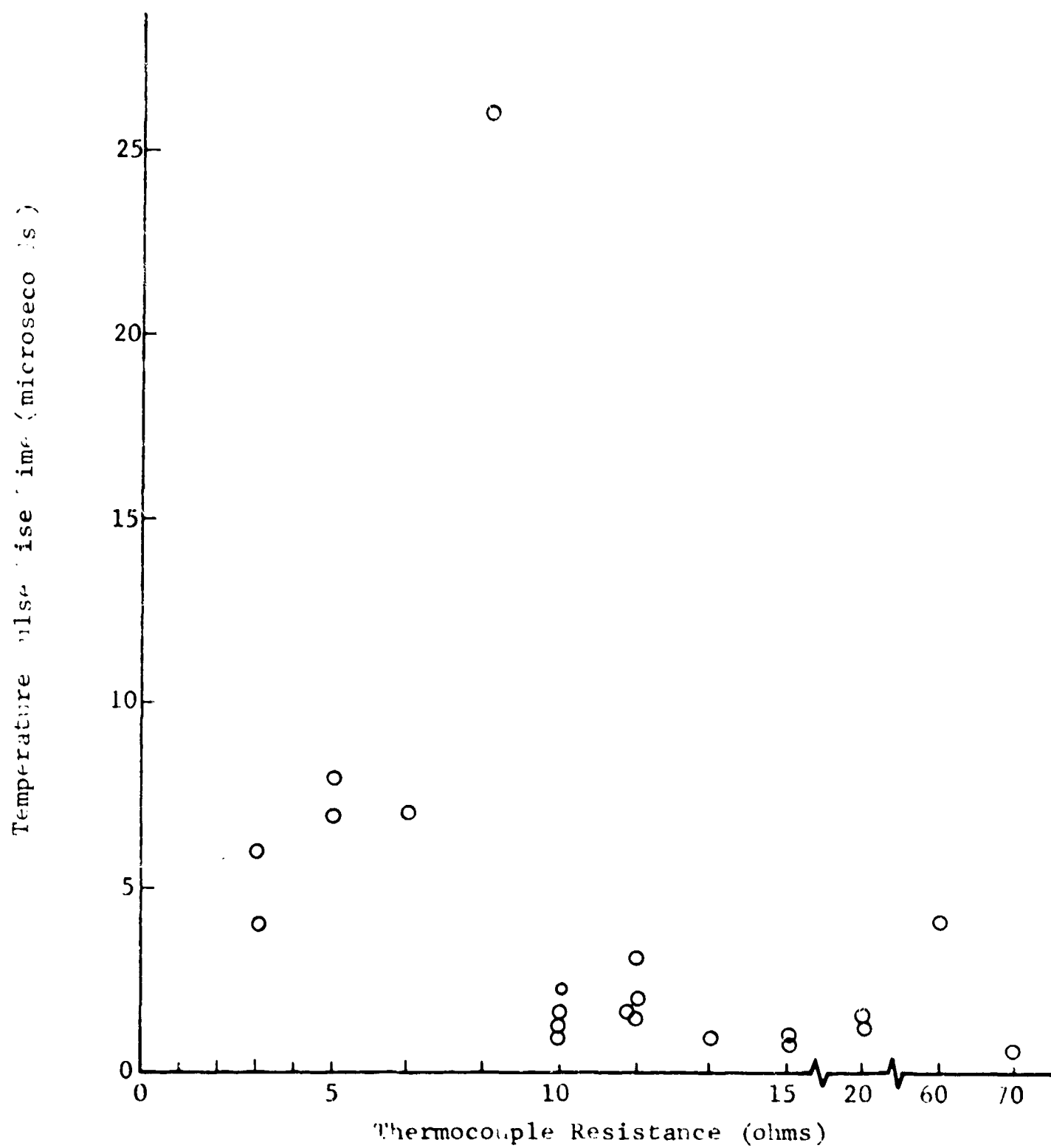
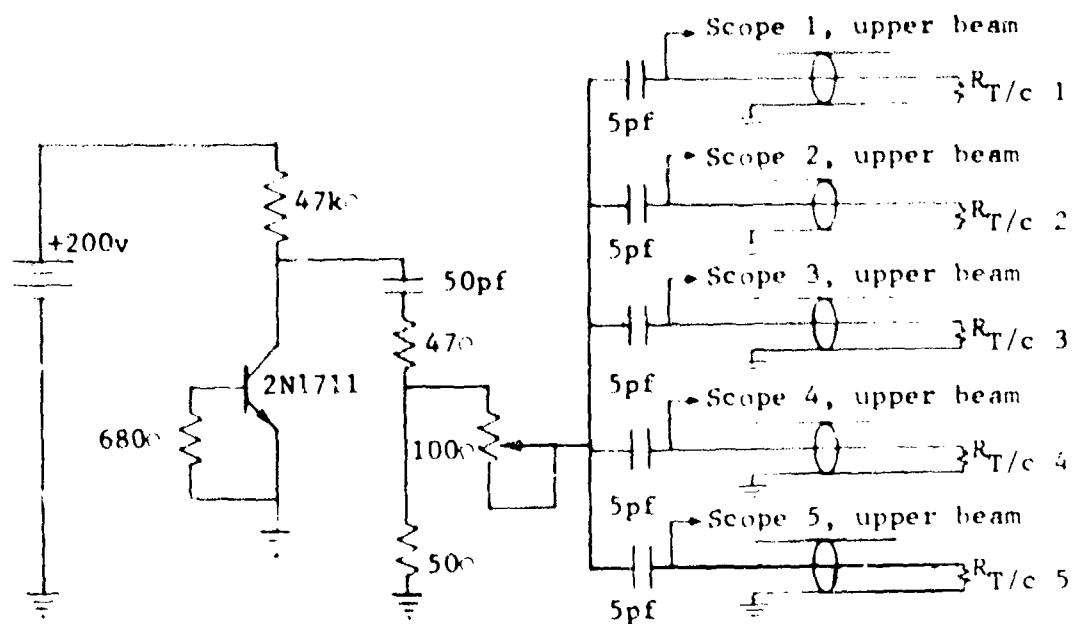


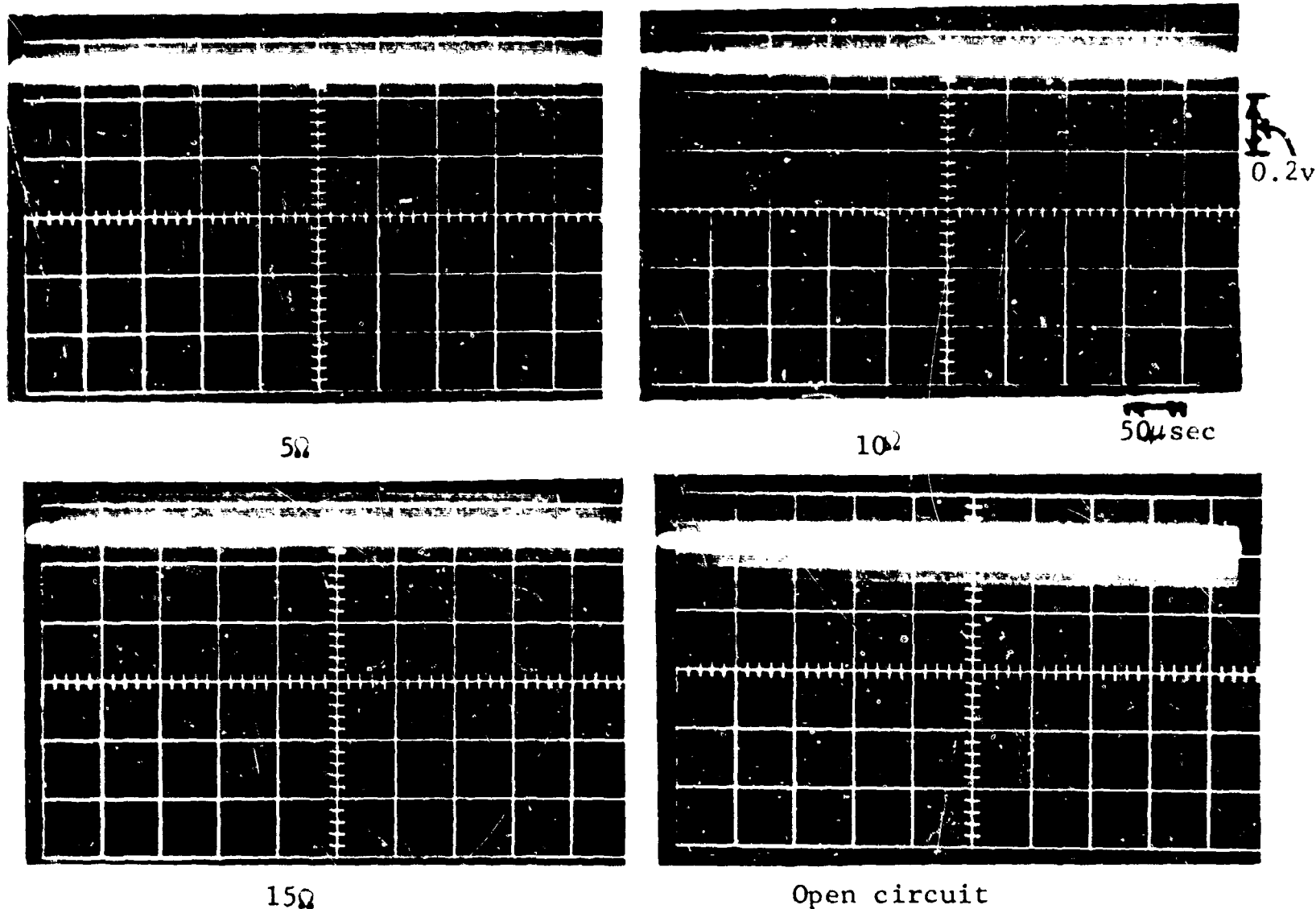
Figure 7. Response time as a function of thermocouple resistance

samples. Most samples in these instrumented experiments were 1/4 inch thick. Further, 90010 plastic bonded mock explosive (an inert material with mechanical properties close to those of PBX 9404) was used in most of the experiments to remove the risk of destroying an anvil plate and a set of thermocouples due to detonation of the sample in an early test. Only two sets of five thermocouples each were available to us. Again, to avoid excessive stress on the anvil plates and thermocouples in early tests, experiments were conducted at low impact velocities.

As mentioned earlier, there was a question as to whether significant abrasion of the thermocouple junctions would occur as a result of extrusion of the explosive over the surface thermocouples. If such abrasion should occur, the junction might be made thicker or thinner in the process, and the response time of the thermocouple would change correspondingly. If response time were degraded substantially for this reason during the extrusion flow, the thermocouple would become incapable of closely following the surface temperature history at its location, and its output would be incorrect and misleading. Since the response time of the thermocouple could be inferred from a measurement of its resistance (see Figure 7), it became desirable to measure the resistance of the thermocouple as a function of time as well as the thermocouple output emf as a function of time during the impact extrusion experiments. Thus, we could determine whether the response time of each thermocouple was short enough to make the indicated temperature histories credible.



(a) Circuit diagram



(b) Calibration record, (halo position denoting reflected pulse amplitude varies as function of thermocouple resistance)

Figure 8 Circuit diagram and calibration records for intermittent monitoring of thermocouple resistance histories.

No means could be devised for measuring the thermocouple resistance directly without introducing unwanted current flows of significance through the delicate junction and interfering with the thermocouple output emf readings. A sampling technique was, therefore, used to measure the resistance at frequent intervals while monitoring the indicated temperature history (output emf) continuously. The circuit by which this was done is shown in Figure 8. The small capacitor bridging the transistor produced regular pulses with a duration of about 0.02 microsecond at intervals of 1 microsecond. The electrical pulse passed along a transmission line to the thermocouple junction and was reflected with an amplitude determined by the resistance of the junction. The sensitivity of this method of intermittently monitoring thermocouple resistance as a function of time was adequate to indicate whether the resistance was unchanged, or had decreased to a low value indicating long response time, or had become very high indicating a loss of the thermocouple junction. Records illustrating variations in reflected pulse "halo" amplitude as a function of thermocouple resistance are presented in Figure 8.

Tektronix model 555 dual-beam oscilloscopes were used to monitor these experiments. While the thermocouple resistance was sampled and displayed on the upper beam, thermocouple output emf, from which interface temperature could be determined, was monitored continuously on the lower beam.

Thermocouple resistance was observed to remain unchanged or to increase during the impact process. Thermocouples were usually found to be open (i.e., junctions were abraded away) following each experiment.

The results of all impact experiments instrumented with surface thermocouples are summarized in Table I. The data return was inconsistent in this series of experiments, principally because of the delicacy of the thermocouple junctions and the low thermocouple output signal (5 to 30 mv) in proportion to oscillatory electrical noise. Thermocouple resistances prior to experiments were in the range of 8 to 30 ohms

Only those oscilloscope records which indicated a rather distinct temperature pulse were listed in Table I. Because of mechanical vibration of the sensors under impact, electrical noise of significant amplitude was superimposed on the signals. The noise reduced the accuracy of temperature readings, which are therefore presented as approximate values in Table I.

The data presented in Table I appear to be consistent with the analytical conclusion that temperature rise should be largest near the outer periphery of the sample. The analytical flow models also indicate that the temperature rise at the center of the sample should be small. While significant temperature pulses were noted at the center thermocouple position in three shots listed in Table I, the center thermocouple appeared to produce credible traces which showed quite small temperature rises in other shots.

After shots on the 90010 mock explosive samples, the 6-inch diameter 0.250-inch-thick sample was found to have been crushed to a thickness of less than 0.2 inch and the edges of the sample were consistently broken away such that its final diameter was ~3 inches. Chips of the broken 90010 mock sample were found scattered in a radius of 20 feet or more about the shot point, where they had flown upon being extruded by the force of the impact.

Table I

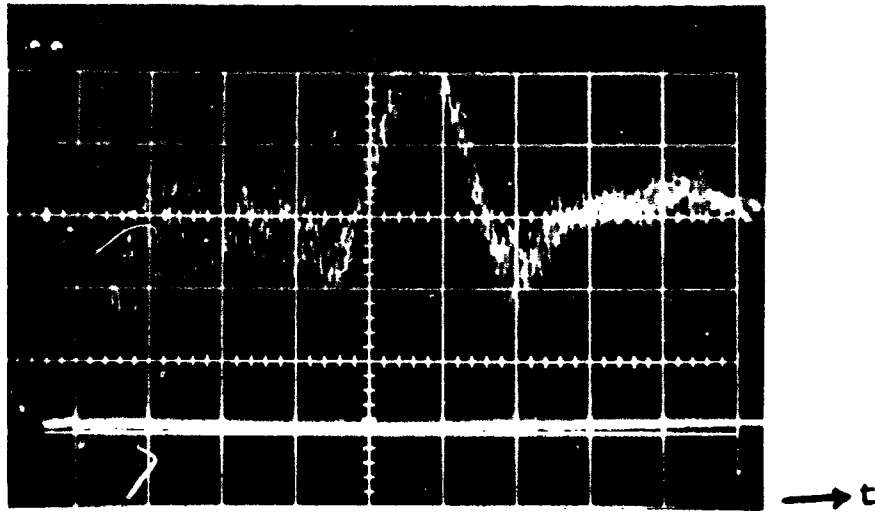
RESULTS OF IMPACT EXPERIMENTS INSTRUMENTED WITH SURFACE THERMOCOUPLES

Shot No.	Sample Material	Sample Thickness (in.)	Estimated Impact Velocity (fps)	Thermocouple Signals			
				Radial Position*	Peak Temp. Rise (°C)	Time of Occurrence (μsec)	Temp. Pulse Duration (μsec)
1	90010 Mock	0.250	255	Int'med. (2) Int'med. (4)	300 300	800 1000	500 300
3	90010 Mock	0.250	255	Outer (5) Outer (1) Center (3)	>250 370 180	25 50 25	150 150 50
6	90010 Mock	0.250	255	Outer (5) Outer (1)	350 700	25 25	100 75
7	90010 Mock	0.250	500	Outer (5) Outer (1) Int'med. (2) Center (3)	850 700 500 700	25 25 25 0	150 800 300 150
8	90010 Mock	0.250	680	Outer (1) Center (3)	1400 1100	20 0	75 1000
9	PBX 9404	0.250	500	Outer (1)	700** 700***	0** 120***	100** 250***

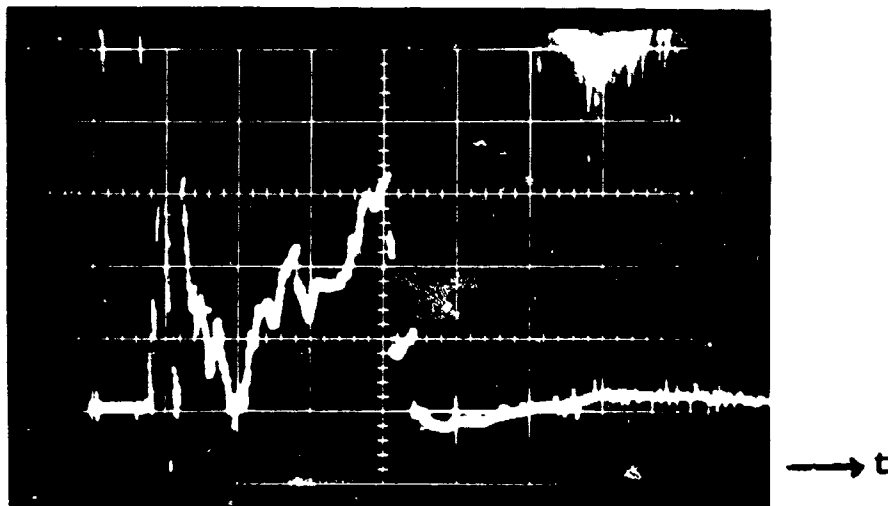
* Number given in parentheses indicates thermocouple position per Figure 5

** First temperature excursion

*** Second temperature excursion (Figure 9).



- (a) Upper trace is emf output from T/C 4, Shot 1.
 Vertical scale: 5 mv/cm, ~equivalent to
 temperature rise of 125°C/cm
 Horizontal scale: 200 μ sec/cm



- (b) Lower trace is emf output from T/C 5, Shot 9.
 Vertical scale: 10 mv/cm, ~equivalent to
 temperature rise of 250°C/cm
 Horizontal scale: 100 μ sec/cm

Figure 9 Oscilloscope records of impact extrusion experiments

The following interpretation of the results reported in Table I is suggested. The radially outermost elements of the impacted sample experience flow at high velocities at the earliest time. These elements are broken up and extruded radially from beneath the driving plate. The temperature pulse experienced at the outer thermocouple location then ends because there is no longer a continuum of material over it. Subsequently, this process is repeated at the radially intermediate thermocouple position, but the flow velocities are lower because of the smaller radius and temperature pulses are correspondingly lower, occur later, and are of longer duration.

In all experiments with inert (90010 mock explosive) samples, temperature pulses resembled that shown in Figure 9(a), i.e., a trace which reached a peak then dropped back down to the base line. In Shot 9, however, where the PBX sample was consumed in a mild reaction, the observed temperature trace shown in Figure 9(b) exhibits a second temperature excursion. This second temperature pulse is believed to represent the liberation of heat by reacting explosive. This diagnostic instrumentation thus appears to be capable of observing the time and approximate location of initiation of ignition.

Shots 8 and 9 cracked the anvil plates in two and destroyed both sets of thermocouples, causing the experimental phase of this work to be terminated, according to plan.

3. Operational Notes

The orientation of the linear thermocouple junctions was arranged to be parallel to the radial direction of flow for some thermocouples, and arranged perpendicular to the direction of flow for other thermocouples, as may be noted in Figure 5. However, no effect of junction orientation upon thermocouple performance was noted in impact extrusion experiments.

The vibrations of the anvil under impact caused tensile failure of the riveted fiber terminal disc on the thermocouple base in early tests. This problem was eliminated by subsequently surrounding the thermocouple base with castable silicone.

III. STUDIES TO EXTEND THE APPLICABILITY OF PREDICTING THE VULNERABILITY OF WEAPONS TO IMPACT

The purpose of this phase of investigation was to gather additional data on explosive impact sensitivity in order to improve predictions of vulnerable impact conditions for weapons. In addition, as a means of confirming the validity of the method of making predictions, experiments were conducted on simulated weapon segments consisting of alternate layers of inert and explosive material. The following specific tasks were accomplished in attaining the objectives of this phase.

- The relationships between impact velocity required for initiation and explosive charge size were determined for Comp B-3, 9010 PBX, and 9404 PBX, for two different input pressure pulse shapes, a square wave and a decreasing exponential pulse.
- The effect of a concentrated impact load on explosive sensitivity was investigated.
- The impact sensitivity of two types of detonators was determined.
- The velocity of sound in 9010 PBX was measured and its elastic moduli computed.
- Calculations were performed to predict the sensitivity of explosives contained in configurations consisting of alternate layers of inert and explosive materials. Experiments were conducted to verify the analysis.

A. Experimental Procedures

1. The Explosive Materials

Both live and mock (inert simulant) explosives were used. The live explosives were Comp B-3*, 9010 PBX**, 9404 PBX***. The mock material, 90010, a mechanical simulant

*Comp B-3, Cast material, 60% RDX, 40% TNT

**9010 PBX, 90% RDX, 10% Kel-F3700 elastomer

***9404 PBX, 94% HMX, 3% nitrocellulose, 3% β -chloroethyl phosphate

for the plastic bonded explosives, was used only for the experiments involving temperature measurements. All billets were fabricated by Mason & Hanger at their Pantex Ordnance Plant, Amarillo, Texas.

Comp B and 9010 PBX were selected since impact sensitivity data, i.e., relationship between charge size and impact velocity required for initiations, does not exist for these explosives. Additional experiments were conducted on 9404 PBX for the purpose of extending our knowledge of the behavior of this explosive to impact conditions not considered in the 1961 study (Ref. 1). Furthermore, these explosive materials were selected because considerable weapon test data are available for weapons containing these explosives. Hence, comparisons between predictions based on IITRI's laboratory data and actual weapon test results can be made, thus enabling a critical evaluation of the validity of the method for making predictions.

The billets were 6 inches in diameter. Selection of this size was based on results of previous IITRI studies (Ref. 1) concerning the effect of billet diameter on the impact sensitivity of 9404 PBX. This work showed that, at diameters greater than $\sim 3\text{-}3/4$ inches, the results are independent of billet diameter. Thus, for the work reported here, the 6-inch billet diameter was considered a reasonable choice, with allowance for a Comp B-3 or 9010 PBX diameter effect greater than the 9404 PBX previously studied. Four different lengths of explosives were tested; $1/4$, $1\text{-}1/2$, 3, and 6 inches. The object of testing different lengths was to determine the relationship between charge length and impact velocity required for initiation. Also, a "limiting" charge length was sought, i.e., the length of explosive such that a further increase in length will not require an increase in impact velocity for initiation of a reaction. Previous work led us to expect the existence of this "limiting" length within the range of sizes tested (Ref. 1, 3).

Two different detonators, IE23 and IE26, used in weapons were impact-tested. The object of impact testing detonators was to compare their response to impact with that predicted by calculations based on empirically derived data on laterally unconfined explosive billets.

2. Experimental Arrangement

In the basic experiment a 6-inch-diameter, 1-inch-thick steel driver plate, is propelled by the uniform initiation of a low density ($\rho = 1 \text{ g/cc}$) tetryl explosive charge placed in contact with the plate. The driver plate uniformly impacts the explosive test specimen*. The impact velocity of the plate varies directly with the quantity of the driver charge used, when the plate size is kept constant. The explosive billet rests on three expendable witness plates, each 12 inches by 12 inches by 1 inch thick. The witness plates, in turn, rest on a steel base or anvil 2 feet in diameter by 2 feet high.

There were some variations in this basic test configuration. For example, for tests where camera coverage was used the base or anvil was approximately 1 foot in diameter by 3 feet high. A 3-inch thick driver plate was used for the laminate configurations. The 3-inch thick plate was also used for experiments to verify that the sensitivity of explosive billets could, in fact, be characterized by impact velocity as the sole parameter and did not depend upon the driver plate weight. The specific test configurations will be detailed in the appropriate section of this report.

* It is the initiation of the low-density tetryl explosive almost simultaneously over its surface that results in the plate being uniformly accelerated. This initiation is accomplished by the fragmentation of an aluminum disk, which occurs when the booster is ignited by a blasting cap. The fast-flying, hot aluminum fragments strike the tetryl explosive driver charge in a large number of places simultaneously and cause the driver explosive to detonate, as illustrated in Figure 2.

3. Criteria of Fire

The criteria by which we concluded that an explosive reaction had occurred were based on visual observation of the damage done to the steel witness plate placed directly beneath the sample being tested. A shot for which no reaction was considered to have occurred left a quantity of unreacted explosive material on the witness plate. If no explosive could be found on the witness plate and if the witness plate surface was not damaged or marred, a consumed (or burning) reaction was considered to have occurred. The criterion for a detonation required that the witness plate show evidence of surface marring such as metal flow, bulging or dishing of the plate. No other criterion was used to determine the intensity of the reaction.

Confidence in using visual inspection as a means of determining the violence of the reaction is based on previous work (Ref. 1,2) where high-speed framing and streak cameras were used to observe impact and subsequent initiation of the explosive billet. In general, witness plate appearance correlated with camera observations. However, witness plate appearance is a more reliable basis for marginal reactions. For example, the smoke from a mild burning reaction occurring in only part of the explosive may completely obscure the field of view during the writing time of the camera. Such a reaction may die out and not propagate to all the explosive material. After the test, small amounts of explosive remain on the witness plate. If one used camera coverage only, the reaction would be classed as a burning reaction. Inspection of the witness plate after the test would show unreacted material, however. This example shot should therefore be classed as a no-go based on the fact that some material remained. High-order detonations, on the other hand, are unambiguous. Witness plate inspection, coupled with experience, provides a reasonably reliable method for interpreting test results.

Recent sensitivity studies by Liddiard and Jacobs at NOL (Ref. 19), involving high-speed camera observations of fireballs* from marginal or subdetonation reactions, indicate that the fireball velocity and growth rate may, when properly interpreted, be the parameter that will enable accurate determination of the amount of material undergoing reaction. If only part of the material reacts, one would expect some asymmetry of the fireball profile. The work of Liddiard and Jacobs holds the greatest promise of providing a quantitative measure of the intensity or extent of subdetonation reactions.

4. Velocity of Sound Measurements

Acoustic techniques were used to measure the velocity of sound in 9010 PBX. This parameter is required in making the prediction calculation. Sound velocity data already exist for Comp B-3 and 9404 PBX (Ref. 2,20). From the measured velocity values, the elastic moduli for 9010 PBX was determined. Elastic moduli M are related to the sound velocity c , and density ρ by

$$M = \rho c^2$$

The modulus under consideration will depend on the type of wave propagated. A plane progressive wave, having a very large beam width compared with a wavelength, will yield the plate modulus B . If the lateral extension of the medium is very small compared with a wavelength (a thin rod), propagation is governed by Young's modulus E . Care has to be taken in both of these situations, as other modes can exist in finite solids. Thin rods will also support surface waves and wide rods will support many modes which bounce from side to side. Shear waves, in general, are well behaved and can, in principle, be propagated in a pure form.

* The fireball is the cloud of smoke or gaseous products seen emerging from a reacting or decomposing explosive.

Several measuring techniques may be used to measure sound velocity, these are:

- (1) phase difference at opposite ends of a block when a wave passes through it,
- (2) refraction effects at interfaces of the unknown solid and a liquid medium of known or readily measurable properties,
- (3) resonance method,
- (4) time-of-flight method.

The time-of-flight method was selected since previous measurements on plastic bonded explosives (Ref. 2) showed that this method yielded consistently credible data, and required relatively little specialized equipment at the test site.

General method of measurement. The velocity of sound is measured by determining the time taken by a physical wave to travel a known distance through the sample. The pulser produces a large voltage across the face of a crystal, which converts the voltage to a pressure on the sample. Since the rise time of the pulse is considerably smaller than a fourth of a period, the crystal does not track the electrical input with a corresponding pressure pulse. Rather, the crystal rings at its resonant frequency, with only a small admixture of harmonics. One might think that mostly harmonics would be present, but a crystal is most sensitive to the resonant frequency. In addition, an oscilloscope display of crystal response showed an almost pure sine wave at the fundamental frequency. Thus, the frequency of the wave traveling in the sample is the resonant frequency of the crystal, rather than some frequency related to the rise time of the electric pulse.

A receiver crystal, with the same resonant frequency as the sender, converts the pressure pulse into a voltage, which is pre-amplified, and displayed on an oscilloscope. Also displayed on the oscilloscope is the output pulse of the

pulser. The time difference between the input pulse and the start of the proper response of the receiver system is found by noting the displacement on the screen of the oscilloscope. The sweep rates on the oscilloscope were calibrated immediately after the experiment, and found to be as indicated by the manufacturer--to 1 per cent accuracy for the portion of the oscilloscope face used in the experiment. Thus, the time between electrical excitation and response was measured. The correction for delays in the crystals themselves, and in the electronic equipment, was found by bonding sender and receiver crystals together, as they are bonded to the samples, and measuring the time between excitation and response.

It might be argued that the proper method of measuring the velocity is to measure the time difference between samples of different lengths. This would unambiguously correct for any electronic and transducer delays. Unfortunately, by ignoring measurements at intermediate lengths, this method loses information.

All samples were 3 in. in diameter, with the sidewalls made nonuniform to reduce coherent reflections. The ends to which the crystals were mounted were flat and parallel.

Measuring the compressional wave. The compressional wave is excited with a 2-in.-diameter ceramic transducer and received with a similar transducer. Each is bonded to the sample with stopcock grease, which will transmit compressional waves. Since the compressional wave travels through the sample faster than any other physical wave, the first wave to hit the receiver is that compressional mode which travels straight down the sample. The time delay, found by noting the time difference when the crystals are bonded together, is less than $0.2 \mu\text{sec}$. Thus, no correction is needed for the measured travel times, since reading of travel time cannot be made to a precision of $0.2 \mu\text{sec}$. Measurement error due to instrumentation is estimated at less than 3 per cent.

Measuring the shear wave. The shear wave is excited with special shear ceramic transducers 1-1/2 in long and 1/4 in. wide and received with a similar crystal. The resonant frequency of each crystal is 100 kc. The crystals are bonded to the explosive with stopcock grease.

Since there is some compressional wave excited by the crystal, a small signal appears first on the oscilloscope. This is checked to be the compressional wave by noting the time at which it is received. Later, a shear wave reaches the receiver and appears as a larger signal. The time at which this larger signal appears is noted. The attenuation of the shear waves is greater than that of the compressional waves. Therefore, the longer samples can have a smaller ratio of shear to compressional waves at the receiver, even though the shear wave is excited with a greater amplitude than the compressional wave. Correction for time delays is found again by gluing the two crystals together, this time with paraffin, and by noting the time difference between excitation and response.

5. Driver Plate Velocities

Driving plate velocities were not measured for each shot since this experiment had been calibrated in previous research programs (Ref. 1, 2) using the same experimental arrangement. Calibration curves which give the relationship between plate velocity and tetryl driver charge weight, for a given driver plate size, are used to determine the impact velocity for the initial conditions of each test.

B. Results of Experiments

1. Planar Impact Loading

The relationship between charge size and impact velocity was determined for 9010 PBX and Comp. B-3. A limited number of experiments was repeated on 9404 PBX to verify that the 1961 results could be duplicated, hence

meaningful comparisons could be made between the several explosives studied. The effects on sensitivity of two slightly different test arrangements were evaluated. In one case, the driver plate, which impacts and subsequently crushes the explosive, is initially in contact with the test explosive. In the second case, there is a 1/2-inch air gap or stand-off between the driver plate and the test sample, Figure 10.

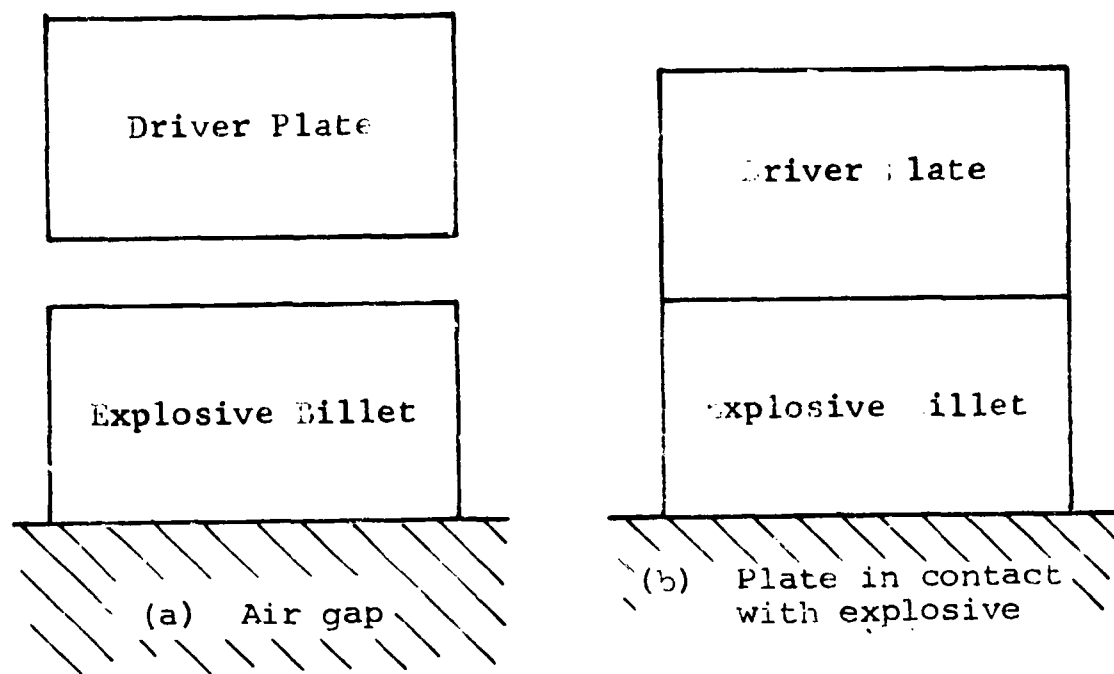


Figure 10 Configurations for planar impact experiments, prior to acceleration of driver plate

When the plate is in contact with the explosive billet the shape the pressure-time pulse at the explosive surface is that of a decreasing exponential function. In the case where there is initially an air gap between the plate and explosive, the shape of the input pressure pulse is that of a square wave or flat top pulse.

Influence of input pressure pulse shape on sensitivity.

The shape of the input pressure pulse for low velocity impact in previous studies (Ref. 1,2) had not been observed to be a variable. The previous work had been done on 9404 PBX,^{*} LX-04,^{**} and RX-04,^{***} all HMX-based materials. In these studies the sensitivity of the HMX-based explosives remained the same under both impact conditions, i.e., the plate initially in contact with the explosive or the plate traveling through an air gap prior to impact. It is generally a more convenient arrangement to have the plate in contact with the explosive. However, when camera coverage is used the air gap configuration is preferred, because the motion of the plate across the gap can be followed and the exact time of impact can be determined. In the present study, it was observed that the air gap configuration resulted in a considerable increase in impact sensitivity of 9010 PBX and a slight increase in Comp B-3 sensitivity. Since the presence or absence of the air gap had not been found to be a significant factor in impact sensitivity experiments on HMX-based explosives, we did not originally intend to systematically evaluate this matter. When this unexpected factor presented itself within the course of work, it was necessary to establish its significance and determine the magnitude of its effect.

* 9404 PBX, 94% HMX, 3% Nitrocellulose, 3% β -chloroethyl phosphate

** LX-04, 85% fine HMX particles, 15% Viton A

*** RX-04, 85% coarse HMX particles, 15% Viton A

Therefore, experiments were systematically carried out to resolve the question of the "irregular" behavior of 9010 PBX and CompB-3. The results of these experiments showed that 9010 PBX was, in fact, strongly affected by the air gap geometry and Comp B-3 only slightly affected. Impact experiments were also carried out on 9404 PBX. The results confirmed the previous observations (Ref. 1,2) that the sensitivity of 9404 PBX is not affected by the air gap configuration. These results are shown in graphical form in Figure 11 and detailed in Table II.

Discussion. Results of experiments employing the two pulse shapes have application in the analysis of the impact vulnerability of weapons. The presence of an air space adjacent to the explosive in a weapon is a frequent occurrence. The effect of this air space may now be taken into account for the explosive materials investigated thus far. If the explosive in a particular weapon is not one of those for which we have data, then the data on the behavior of the most sensitive explosive, 9010 PBX, should be considered as the applicable data for safety purposes.

The shape of the input pressure pulse has only within recent years been suggested as a possible variable in sensitivity studies. There has been practically no work done in this area. A systematic study on 9404 PBX at LASL (Ref. 21) was concerned with the effect of very short duration square wave pressure pulses on the time delay to high-order detonation. Marlow (Ref. 22) has investigated the effect of divergent waves from a thin rod on the initiation of an HMX/TNT composition. For the two pulse shapes considered

Impact Velocity (fps)

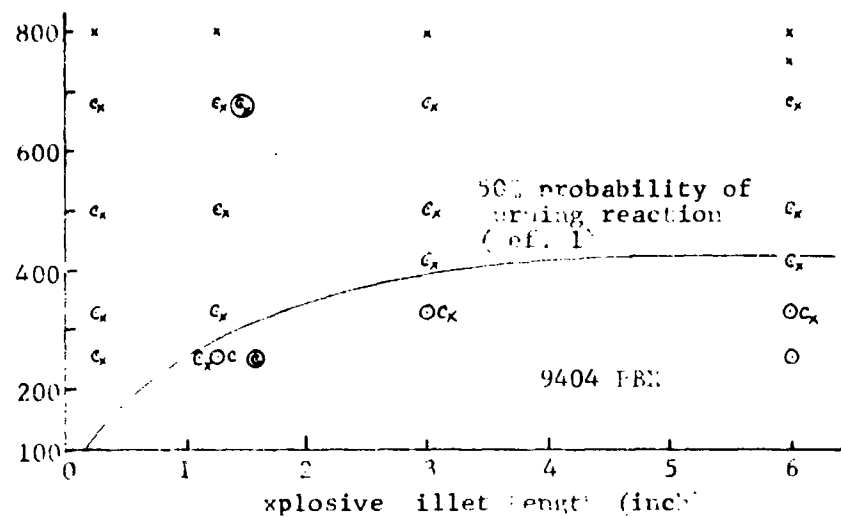
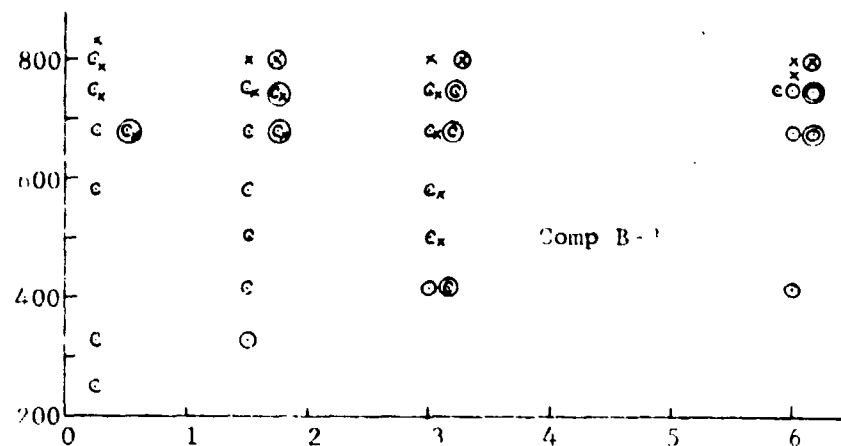
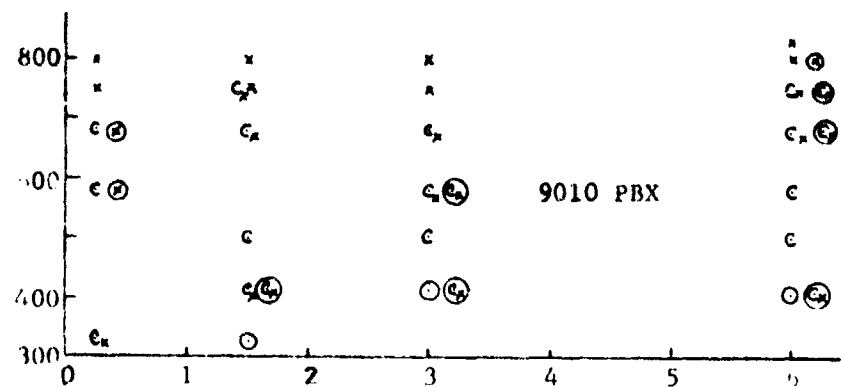


Figure 11 Results of planar impact experiments, various lengths of explosives

Note: Circled data points represent results of tests employing air gap configuration (Figure 10)

Table II
SUMMARY OF PLANAK IMPACT EXPERIMENTS

Driver Plate In Contact With Explosive				Air Gap Initially Between Driver Plate And Explosive			
Shot No.	Billet Height (in.)	Impact Velocity (fps)	Results, witness plate appearance	Shot No.	Billet Height (in.)	Impact Velocity (fps)	Results, witness plate appearance
152	0.25	330	Cx 3/8" dent in W.P.				
31	0.25	580	C, slight dent in W.P.	95	.25	580	X, deep dish in W.P.
24	0.25	680	C, slight dent in W.P.	77	.25	680	X, H.O. detonation
45	0.25	680	C, slight dent in W.P.				
32	0.25	750	X, H.O. detonation				
30	0.25	800	X, H.O. detonation				
8	1.5	330	0, explosive left on W.P.				
153	1.5	415	Cx, 1/2" dent in W.P.	65	1.5	415	Cx, 3/4" dent in W.P.
26	1.5	500	C, slight concave effect				
10	1.5	680	Cx, 3/4" dent in W.P.				
28	1.5	750	Cx, 3/4" dent in W.P.				
46	1.5	750	X, H.O. detonation				
33	1.5	800	X, H.O. detonation				
6	3.0	415	0, explosive on W.P.	67	3.0	415	Cx, 1/2" dent in W.P.
22	3.0	500	C, slight dent in W.P.				
12	3.0	580	Cx, 3/4" dent in W.P.	78	3.0	580	Cx, 3/4" dent in W.P.
2	3.0	680	Cx, 3/4" dent in W.P.				
14	3.0	750	X, H.O. detonation				
4	3.0	800	X, H.O. detonation				
16	6.0	415	0, explosive on W.P.	68	6.0	415	Cx, 3/4" dent in W.P.
34	6.0	500	C, slight concave effect				
25	6.0	580	C, slight concave effect				
35	6.0	680	Cx, 3/4" dent in W.P.	79	6.0	680	Cx, 3/4" dent in W.P.
18	6.0	750	Cx, 3/4" dent in W.P.	96	6.0	750	Cx, very deep dish in W.P.
20	6.0	800	X, deep dent	122	6.0	800	X, H.O. detonation
47	6.0	830	X, H.O. detonation				

Table II (Cont.)

6-in.-diam 9010
6-in.-diam by 3-in.-thick Driver Plate

Driver Plate In Contact With Explosive			Air Gap Initially Between Driver Plate And Explosive				
Shot No.	Billet Height (in.)	Impact Velocity (fps)	Results, witness plate appearance	Shot No.	Billet Height (in.)	Impact Velocity (fps)	Results, witness plate appearance
155	0.25	680	5/8" dent in W.P.				
57	1.5	150	C , slight dent in W.P.				
58	3.0	150	0 , explosive on W.P. 0 , explosive on W.P. 0 , explosive on W.P. 0 , explosive on W.P. C , clean W.P. C , slight dent in W.P.	60	3.0	150	Cx, deep dent in W.P. Cx, deep dent in W.P.
125	3.0	415		61	3.0	150	
130	3.0	415					
131	3.0	415					
134	3.0	415					
128	3.0	500					
154	6.0	415	Cx, 3/4" dent in W.P.				

Table II (Cont.)

6-in.-diam Comp B-3
6-in.-diam by 1-in.-thick Driver Plate

Driver Plate In Contact With Explosive			Air Gap Initially Between Driver Plate And Explosive				
Shot No.	Billet Height (in.)	Impact Velocity (fps)	Results, witness plate appearance	Shot No.	Billet Height (in.)	Impact Velocity (fps)	Results, witness plate appearance
156	0.25	255	C, clean smooth W.P.				
147	.25	330	C, slight dent in W.P.				
36	.25	580	C, slight dent in W.P.				
23	.25	680	C, dent in W.P.	91	.25	680	Cx, 1/4" dent in W.P.
48	.25	750	Cx, 3/4" dent in W.P.				
29	.25	800	Cx, 3/4" dent in W.P.				
49	.25	830	X, deep dish in W.P. almost H.O.				
7	1.5	330	0, HE left on W.P.				
71	1.5	415	C, W.P. clean & smooth				
69	1.5	500	C, W.P. clean & smooth				
37	1.5	580	C, W.P. clean & smooth				
9	1.5	680	C, W.P. slightly concave	80	1.5	680	Cx, 3/4" dent in W.P.
27	1.5	750	Cx, 1/4" dent in W.P.	90	1.5	750	Cx, 3/4" dent in W.P.
38	1.5	800	X, H.O. detonation	92	1.5	800	X, deep dish in W.P. almost H.O.
5	3.0	415	0, melted explosive left on W.P.	66	3.0	415	C, clean smooth W.P.
21	3.0	500	Cx, metal flow on W.P.				
11	3.0	580	Cx, metal flow on W.P.				
1	3.0	680	Cx, metal flow on W.P.	81	3.0	680	C, clean smooth W.P.
1	3.0	750	Cx, 1/2" dent in W.P.	89	3.0	750	C, small dent in W.P.
3	3.0	800	X, H.O. detonation	93	3.0	800	X, H.O. detonation
50	3.0	800	X, H.O. detonation				
15	6.0	415	0, HE left on W.P.				
70	6.0	680	0, HE left on W.P.	72	6.0	680	0, HE left on W.P.
17	6.0	750	0, melted HE on W.P.	82	6.0	750	0, melted HE left on W.P.
39	6.0	750	C, clean W.P.				
148	6.0	780	X, H.O. detonation				
19	6.0	800	X, H.O. detonation	94	6.0	800	X, deep dish in W.P. almost H.O.
51	6.0	800	X, H.O. detonation				

Table II (Cont.)

6-in.-diam Comp B-3
6-in.-diam by 3-in.-thick Driver Plate

Driver Plate In Contact With Explosive			
Shot No.	Billet Height (in.)	Impact Velocity (fps)	Results, witness plate appearance
149	1.5	330	C , clean smooth W.P.
123	3.0	415	0 , HE left on W.P.
126	3.0	500	0 , HE left on W.P.
133	3.0	500	0 , HE left on W.P.
132	3.0	580	Cx, metal flow on W.P.
150	6.0	750	Cx, 1/2" dent in W.P.

Table II (Cont.)

6-in.-diam 9404 PBX
6-in.-diam by 1-in.-thick Driver Plate

Driver Plate In Contact With Explosive				Air Gap Initially Between Driver Plate And Explosive			
Shot No.	Billet Height (in.)	Impact Velocity (fps)	Results, witness plate appearance	Shot No.	Billet Height (in.)	Impact Velocity (fps)	Results, witness plate appearance
97	.25	255	Cx, 1/4" dent in W.P.				
112	.25	255	Cx, 1/4" dent in W.P.				
88	.25	330	Cx, small dent in W.P.				
101	.25	500	Cx, 3/4" dent in W.P.				
103	.25	680	Cx, 3/4" dent in W.P.				
107	.25	800	X , H.O. detonation				
116	.25	800	X , deep dish				
87	1.5	255	0 , HE left on W.P.				
109	1.5	255	C , clean smooth W.P.				
113	1.5	255	Cx, 1/4" dent in W.P.	120	1.5	255	Cx, 1/2" dent in W.P.
73	1.5	330	Cx, 3/4" dent in W.P.				
98	1.5	500	Cx, 3/4" dent in W.P.				
102	1.5	680	Cx, 3/4" dent in W.P.	121	1.5	680	Cx, 3/4" dent in W.P.
104	1.5	800	X , H.O. detonation				
117	1.5	800	X , H.O. detonation				
74	3.0	330	0 , HE left on W.P.				
85	3.0	330	Cx, 3/4" dent in W.P.				
110	3.0	330	0 , HE left on W.P.				
76	3.0	415	Cx, 3/4" dent in W.P.				
114	3.0	415	Cx, 1/4" dent in W.P.				
86	3.0	500	Cx, 3/4" dent in W.P.				
99	3.0	680	Cx, 3/4" dent in W.P.				
105	3.0	800	X , H.O. detonation				
118	3.0	800	X , H.O. detonation				

Table II (Concluded)

6-in.-diam 9404 PBX
6-in.-diam by 1-in.-thick Driver Plate

Driver Plate In Contact With Explosive			
Shot No.	Billet Height (in.)	Impact Velocity (fps)	Results, witness plate appearance
100	6.0	255	0, HE left on W.P.
83	6.0	330	Cx, 3/4" dent in W.P.
111	6.0	330	0, HE left on W.P.
75	6.0	415	Cx, 3/4" dent in W.P.
115	6.0	415	Cx, 1/4" dent in W.P.
84	6.0	500	Cx, 3/4" dent in W.P.
106	6.0	680	Cx, 3/4" dent in W.P.
119	6.0	750	X, H.O. detonation
108	6.0	800	X, H.O. detonation

6-in.-diam 9404 PBX
6-in.-diam by 1-in.-thick Driver Plate

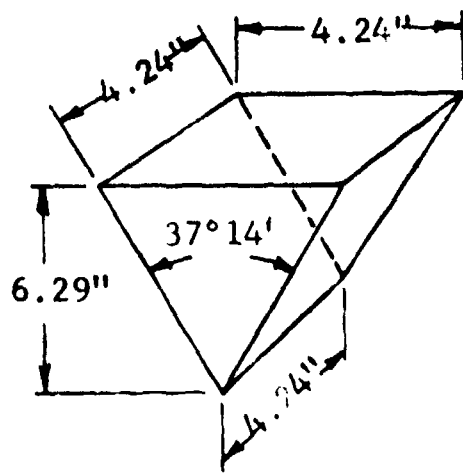
Driver Plate In Contact With Explosive			
Shot No.	Billet Height (in.)	Impact Velocity (fps)	Results, witness plate appearance
124	3.0	330	0, HE left on W.P.
129	3.0	330	0, HE left on W.P.
127	3.0	415	Cx, 3/8" dent in W.P.

in the IITRI experiments we have the same plate mass striking the explosive at the same initial impact velocity. The momentum and energy are the same in both cases: The rate at which the momentum is deposited differs, however. These differences are significant for 9010 PBX, less important for Comp B-3, and unimportant for 9404 PBX. We believe that an understanding of the role of input pressure pulse shape, i.e., the form of the energy deposition, on initiation of subdetonation reactions in explosives is a necessary step in the total understanding of the initiation process.

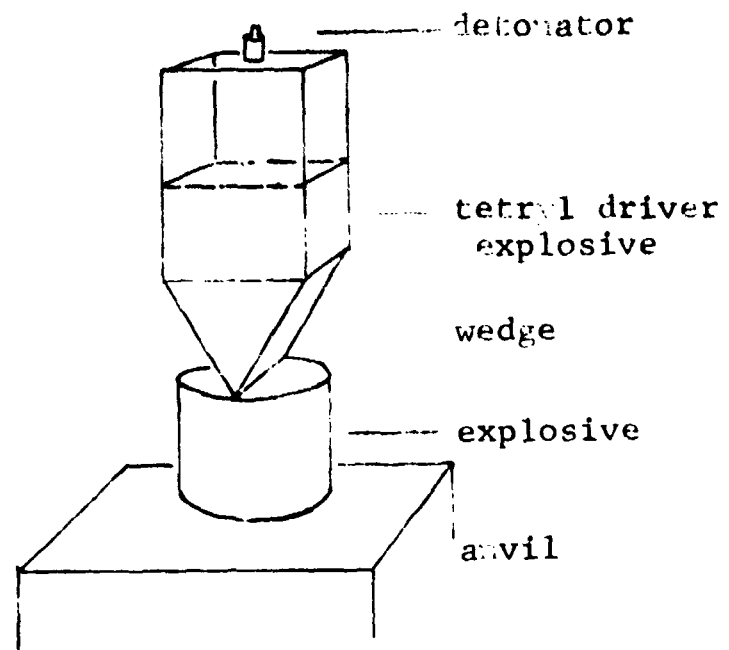
2. Concentrated Impact Loading

The impact sensitivity experiments conducted thus far had been concerned with the effect of a planar uniformly distributed load. It was expected that a more sensitive condition existed if the same energy or momentum of the applied load were concentrated over a smaller volume of explosive. Thus, as a small part of this program, we also considered the effect of a nonuniformly distributed load.

A wedge-shaped loading device was selected since the solution of the penetration of wedge into a target is available in the literature (Ref. 23, 24). Figure 12 shows the shape of the wedge that was used.



(a) Wedge Dimensions



(b) Test Arrangement

Figure 12 Wedge-shaped impact loading device

The weight of the wedge is exactly the same as that of a 6-inch-diameter, 2-inch-thick steel driver plate, 16 lb. The wedge had a sharp or pointed edge, except in one case where the bottom edge was flattened according to Figure 12. The explosives tested, Comp B-3 and 9010 PBX, were 6 inches high. The results of impact experiments, Table III, showed that the wedge impact is not a more sensitive loading condition.

Table III

SUMMARY OF WEDGE IMPACT EXPERIMENTS

6-Inch-Diameter, 6-Inch-Thick Explosive Billet

Shot No.	Explosive	Impact Velocity (fps)	Results	Response of billet if impact load had been uniformly distributed
141	Comp B-3	750	HE broke up into large chunks	Explosive completely consumed
144	Comp B-3	800	HE broke up into large chunks	High order detonation
145	Comp B-3	800	Tip of wedge was flattened to 3/16" width prior to test. Results were same as 141 & 144	High order detonation
142	9404 PBX	530	HE broke up into small pieces	Less than 50% probability of burning reaction
143	9404 PBX	680	1/4" dent in W.P., fine HE dust in test area	Deep dent in W.P., low order detonation

No reaction occurred in Comp B-3 at impact velocities that were high enough to cause high-order detonation for a planar impact configuration. Our inability to initiate this explosive clearly shows that caution must be exercised in comparing the response of explosives to different forms of applied energy. It is not only the total amount of energy available that is important, but the means by which the energy is deposited and the mechanism which is operative for that method of energy deposition.

Significance Of Wedge Test Results On Weapon Response

In earlier IITRI work on weapons containing plastic bonded explosives (Ref. 4), the predicted values of the critical impact velocity for initiation were within 20 percent of the experimentally bracketed values for six of the seven weapon types for which predictions were made. The seventh weapon was found to be more sensitive than had been predicted. In this case, an extremely concentrated local loading condition, unlike the laboratory impact experiment upon which the prediction was based, appeared to be responsible for the increased sensitivity and, hence, for the inaccuracy of the prediction. Uniformly distributed loading had been implicitly assumed in the prediction calculations. Deformation, which occurs over a small area or sharp line on contact, causes much higher stresses in these regions than the same force would cause if it were operating over a large area. However, the wedge test results show that one cannot know in advance whether a given concentrated load will, in fact, be a more sensitive configuration, in spite of the higher stresses developed in the explosive. Thus, if the explosive in a weapon can be subjected to a concentrated or stab-type loading, response of the explosive to such a load must be determined by experiments which simulate this concentrated load. One can only successfully predict the response of weapon systems to impact if the valid assumption that the same mechanism is responsible for initiation in both

laboratory experiments and the accidental weapon impact is valid. To make reliable predictions of vulnerable impact conditions solely by analytical means, we must be able to understand the processes which are active during impact initiation and the mechanisms governing these processes. Solution of the wedge penetration problem for the case of an explosive target is a good example of one problem that can be pursued analytically using available theoretical techniques.

3. Sensitivity of Detonators

Two different detonators IE23 and IE26 were impact-tested during this program. The purpose of these tests was to verify that the method used to predict the impact sensitivity of detonators is valid. Detonators are of a much smaller diameter than the billets presently being tested, (although unconfined 9404 PBX billets as small as 1-1/2 inch diameter were impact-tested in an earlier program (Ref. 1)). The HE in the detonators are confined in plastic and metal containers whereas all our sensitivity testing was on unconfined billets. The results of these tests, listed in Table IV, are not consistent. The reason for this inconsistency is not understood, since, as far as we can tell, there were no differences in the procedure for carrying out these experiments. In all cases the detonators rested on a 6-in.-diam steel base, and were impacted by a 1-1/2-in.-diam by 1-1/4-in.-high steel driver plate. The plate velocities for all tests ranged between 150 fps to 275 fps. The maximum velocity attainable for the 1-1/2-in.-diam system is 275 fps. Our predictions indicate that 150 fps should be sufficient to initiate the IE23 detonator. Unless the anomalous behavior of the detonators is resolved, the results are of no significance. The irregular behavior of the detonators may be due to the fact that more than one mechanism for initiation can occur

Table IV
IMPACT EXPERIMENTS ON DETONATORS

1E 26 Detonators			1E 23 Detonators		
Shot No.	Plate Impact Velocity(fps)	Results, witness plate appearance	Shot No.	Plate Impact Velocity(fps)	Results, witness plate appearance
1	195	C, W.P. clean, complete burn	4	195	C, W.P. clean complete burn
2	265	C, W.P. clean, complete burn	7	160	0,
3	170	C, W.P. clean, complete burn	8	170	0,
5	150	0,	10	195	0, HE and detonator fragments remained
6	160	0,	14	225	0,
9	170	0, HE and detonator fragments remained	15	250	0,
11	200	0,	16	275	C, W.P. clean complete burn
12	225	0,	18	260	C, small piece of HE remained
13	275	C, W.P. clean, complete burn			
17	250	C, W.P. clean, complete burn			

in a confined system. The mechanism that is operating in a particular experiment may be related to the mode of failure of the confining case.

4. Velocity of Sound in 9010 PBX

The results of the measurements of sound velocity and the elastic constants of 9010 PBX are given in Table V.

Table V

SOUND VELOCITY AND ELASTIC CONSTANTS OF 9010 PBX

Average density, ρ :	1.787 gm/cm ³
Compressional velocity, c_b :	2702 meters/sec
Shear velocity, c_t :	1330 meters/sec
Plate modulus, B	130.7 10^9 dynes/cm ²
Lame's constant, μ :	31.6 10^9 dynes/cm ²
Lame's constant, λ :	67.5 10^9 dynes/cm ²
Bulk modulus, K:	88.6 10^9 dynes/cm ²
Young's modulus, E:	84.8 10^9 dynes/cm ²
Poisson's ratio, ν :	0.34

The velocities are found by dividing the path length by the corrected time of travel. From these velocities, and from a knowledge of the density of the samples, the elastic moduli are computed from the following equations.

$B = \rho c_b^2$	Plate Modulus
$\mu = \rho c_t^2$	Lame's Constants
$\lambda = B - 2\mu$	
$B = \lambda + 2\mu$	Plate Modulus
$K = \lambda + \frac{2}{3}\mu$	Bulk Modulus
$E = \frac{\mu(3\lambda + 2\mu)}{\lambda + \mu}$	Young's Modulus
$\nu = \lambda / 2(\lambda + \mu)$	Poisson's Ratio

5. One-Dimensional Composites, Analysis and Experiments

Weapon configurations may be simulated by one-dimensional composites consisting of alternate layers of explosive and inert materials. Such model segments may be tested under better controlled conditions than are possible in full-scale field tests of weapons. In this study calculations were made of longitudinal wave motion in layered systems of explosive and inert materials representing a composite of materials encountered in weapon design, in order to determine interactions which may lead to explosive initiation at relatively early times after impact. Predictions were made of critical impact velocities for initiation of the explosive in these simple systems. Experiments were then conducted on one-dimensional composites duplicating the model analyzed to confirm the predictions.

Several composites were analyzed. They consisted of combinations of steel, aluminum, lead, and explosives. Figure 13 shows the configurations which were analyzed. Figure 14 shows the results of the analysis in terms of initial plate velocity and particle velocity at the explosive.

In the previous prediction calculations (Ref. 3,4, 9) all materials were assumed to behave elastically. In an effort to improve the predicted vulnerable impact velocities for initiation of explosives in layered systems the real material properties (equations of state) were taken into account, and wave interactions were computed by means of IITRI's SWIMM Code (Ref. 26). The results of these more rigorous calculations, when compared with the elastic approximation, show that the elastic approximation is sufficiently accurate. A detailed description of the method for predicting the impact response of an explosive material is given in the Appendix. Of the several model configurations the lead-aluminum buffer appears to offer the most sensitive condition. For example, for an impact velocity of 300 fps, the initial particle velocity at

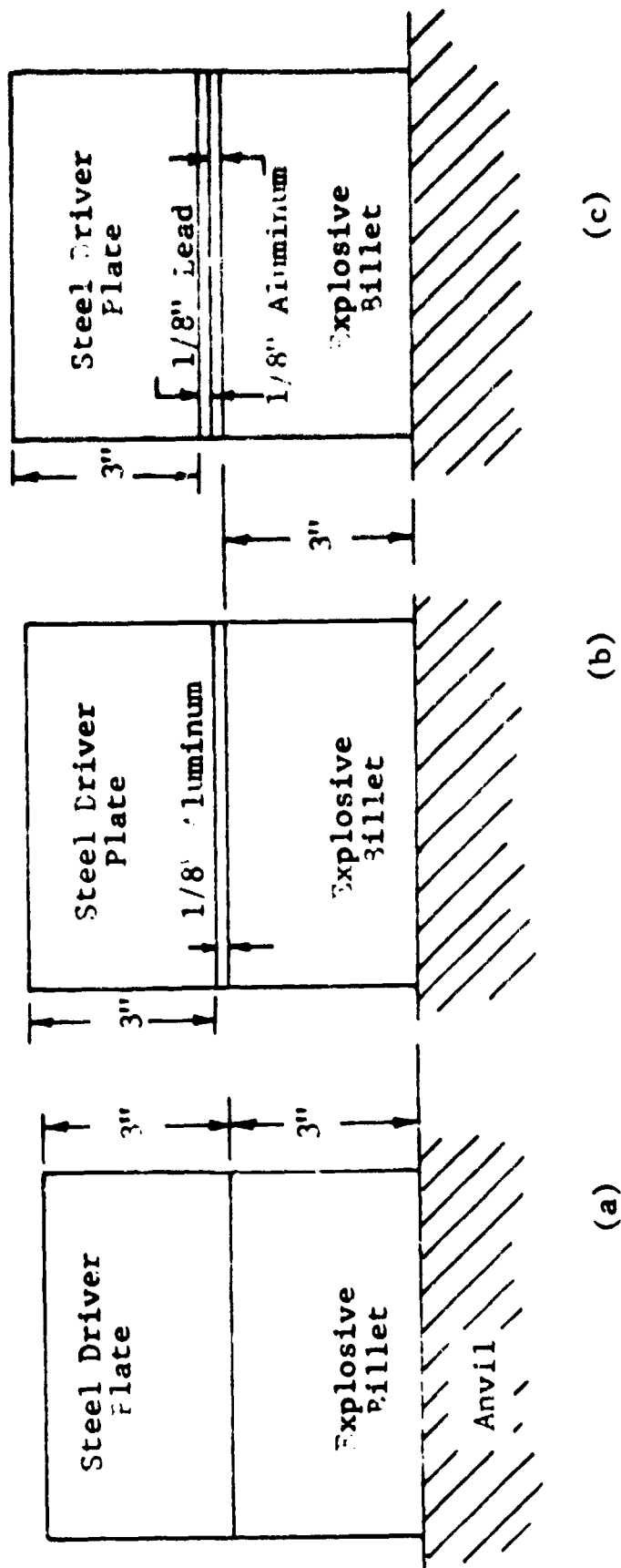
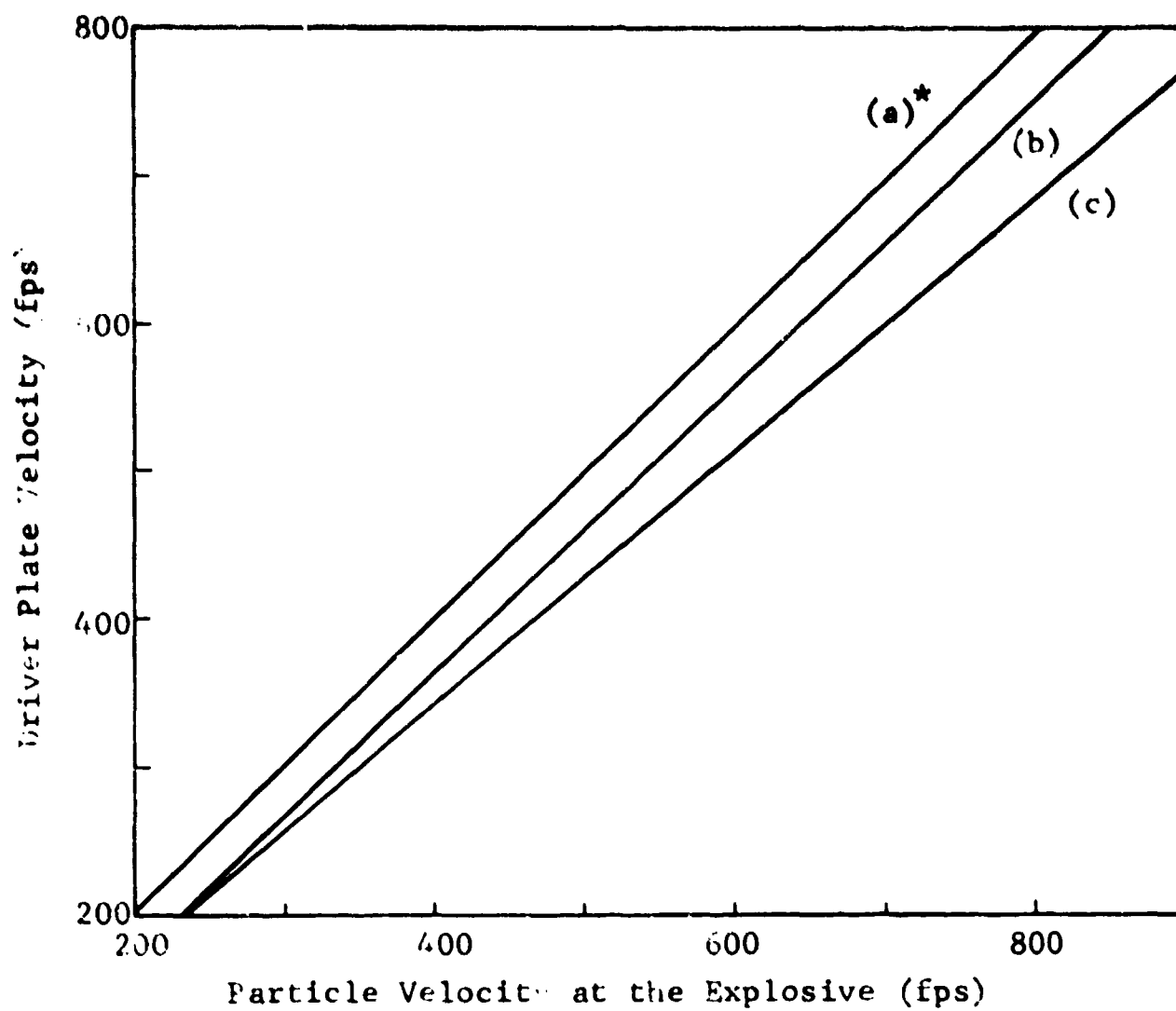


Figure 13 One-dimensional composites used as models for wave propagation calculations and impact experiments to validate prediction technique



* averaged composite shown in figure 13(a)

Figure 14 Computed particle velocity at the explosive, for layered composites detailed in Figure 13

the explosive surface would be 353 fps. The initial test conditions were such that the plate velocity of Shot 140, 415 fps would not be sufficient to initiate the explosive in the absence of the aluminum and lead. However, with the aluminum and lead layers the particle velocity at the explosive 488 fps is sufficient to initiate the explosive as predicted. The other shots also behaved as predicted. The details of the composite experiments, predicted values and results of experiments are given in Table VI. These experiments show that within the limits of the materials considered, the prediction method is valid.

Table VI

SUMMARY OF EXPERIMENTS ON LAYERED MATERIALS

Laminate Configuration, DP, Pb, Al, HE, Anvil As Detailed In Figure 13

Shot No.	Explosive (3-Inch Thick)	Plate Impact Velocity (fps)	Calculated Particle Velocity at HE(fps)	Predicted Results		Actual Results
				Simple DP-HE system	Laminate Configuration	
137	Comp B-3	500	585	0, HE on W.P.	Cx, metal flow on W.P.	C, clean smooth W.P.
139	Comp B-3	500	585	0, HE on W.P.	Cx, metal flow on W.P.	Cx, slight dent in W.P.
146	Comp B-3	750	875	Cx, dent in W.P.	X, H.O. detonation	X, H.O. detonation
140	9010 PBX	415	488	0, HE on W.P.	C, slight dent in W.P.	C, slight dent in W.P.
151	9010 PBX	680	795	Cx, dent in W.P.	X, H.O. detonation	X, H.O. detonation
138	9404 PBX	330	385	0, HE on W.P.	Cx, 1/2" dent in W.P.	Cx, dent in W.P. plate warped

IV. CONCLUSIONS AND RECOMMENDATIONS

The results of the studies carried out on this research program have confirmed the validity of the prediction method (Ref. 3,4,9 and Appendix). The elastic approximation was shown to be sufficiently accurate for predicting the impact sensitivity of explosives in layered configurations which are simple models of weapon systems. The acquisition of additional sensitivity data for Comp B-3, 9010 PBX and 9404 PBX should improve the accuracy of predicted vulnerable impact velocities for weapons containing these explosives. The unexpected insensitivity of these explosives to a concentrated load in the form of a wedge-shaped loading device as well as the various degrees to which explosives are influenced by shape of the input pulse, points out the care that must be exercised in comparing the response of explosives subjected to different forms of applied energy. In spite of this fact, the results of properly designed experiments can be used to predict the response of weapon systems to impact provided the same mechanism governs the explosives response both in laboratory and weapon tests.

Many different mechanisms can govern the response of an explosive to impact. The variables that control the operation of these mechanisms are related to the geometry, composition and environment of the explosive, and the details of the applied load. The precise processes by which an explosive is ignited by low-speed impact are not understood. For example, the experimental observation of high interface temperatures by rapid response surface thermocouples in this study, as had been predicted by flow analyses by ILTRI in this report and by Weston (Ref. 15), represents a significant first step toward pinpointing the ignition mechanism for a single geometry, the pinch condition. Much work remains to be done in confirming and then in utilizing an understanding of the

mechanism of ignition in the pinch condition and other impact situations of importance.

The technique for predicting vulnerable weapon impact velocities, which utilizes laboratory data in a simple longitudinal stress wave analysis, is rather well established. Progress toward a complete solution to the impact problem requires further fundamental study of the low-velocity impact ignition of explosives, however. Rather than doing any further impact tests on specific configurations, work should be directed toward determining the basic processes by which local hot spots of sufficient intensity and size to grow into propagating explosive reactions are developed.

APPENDIX

Model For Predicting Impact Initiation Of The Explosive Component In A Weapon

The results of the laboratory experiments are used in the analysis to predict the vulnerable impact velocity of a weapon or a layered composite representing a weapon section. The data on critical impact velocity as a function of charge size (Figure 1) cannot be used directly for prediction purposes, since the explosive in the system is surrounded by many layers of materials and may strike a variety of target materials not included in the experiments. This does not pose a real limitation inasmuch as the impact sensitivity of the explosive may be characterized by the particle velocity transmitted to the explosive, and we can calculate the manner in which the applied load is modified as the disturbance traverses the unit.

We can, therefore, from knowing the required particle velocity for initiation of the explosive, compute the required weapon impact velocity. Thus, it is somewhat of an advantage to first study the explosive under as simple environmental conditions as possible so that the experimental results are sufficiently general that they can, by proper computation, be applied to many, quite different, weapon configurations.

Upon impact of a weapon against a target, the sudden application of load causes deformations and stresses which are not immediately transmitted to all parts of the body. Remote portions of the weapon may remain undisturbed for some time. The propagation of the disturbance caused by the impact, the stress wave, is modified upon crossing interfaces between different materials.

Thus, as the physical properties of the medium through which the stress wave is propagating change, the pulse will be modified at crossing the change or interface. From the point of application of load to the location, within the weapon, of

the high explosive components, this stress wave crosses several interfaces; consequently, the amplitude of the initial stress and particle velocity will be altered by the time it reaches the explosive. By computing the stress and particle velocity in the explosive as a result of the disturbance resulting from the weapon impacting the target and the large number of wave interactions in the laminates which make up the weapon, one can make predictions regarding the impact vulnerability of the weapon

Method Of Calculation For Elastic Approximation

The pressure and particle velocity behind the stress wave can be calculated directly from the Rankine-Hugoniot jump conditions expressing conservation of momentum. Across an elastic wavefront, this relationship is

$$P = \rho C U_p$$

where

P = pressure or stress normal to the wave front

(kilobars(1 bar = 10^6 dynes/cm²=14.5 psi;
1 kbar= 10^3 bars; 1 Megabar = 10^6 bars)*)

ρ = density (gm/cm³)

C = elastic wave velocity or the sound velocity
(meters/sec)

U_p = particle velocity (meters/sec)

At the boundary between two materials, the pressure and particle velocity must be equal.

Actually a graphical solution called the impedance, or characteristic, method is used for determining the pressure P and the particle velocity, U_p in the explosive. To explain the impedance method, an example, Figure 15, is given which considers only two materials, as in the air gap experiment, a flyer

*A bar - millisecc - gram-cm or a Mbar - microsec - gram-cm system of units, conveniently, does not require a conversion factor.

plate impacting a stationary explosive billet. In this example, a line is drawn through the origin which represents the locus of all (P, U_p) states which can be attained in the stationary billet. This line is constructed by knowing the initial density ρ and sound velocity C of the target (explosive) material. The slope of this line is ρC , since, from the conservation of momentum, $P = \rho C U_p$ or $P/U_p = \rho C$.

When the flyer plate impacts the target, a disturbance or stress wave is reflected back into the plate. The locus of (P, U_p) states, which can be attained behind the reflected wave in the plate, is given by the cross curve. This line is constructed by knowing the initial density and sound speed in the plate material. The slope of this cross curve is ρC . The intersection of the two lines is the state common to both materials and satisfies the boundary condition that P and U_p be equal across the interface of the plate and target.

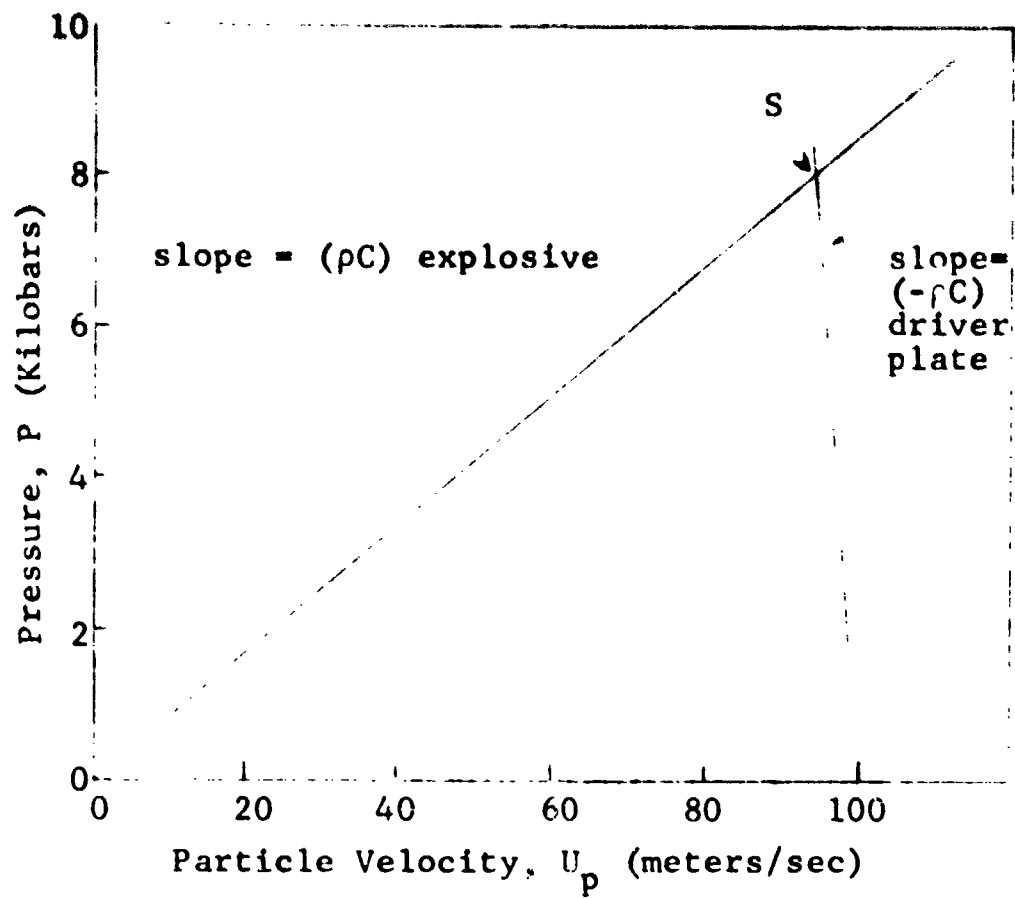


Figure 15 Graphic method for obtaining (P, U_p) at the interface of two materials upon impact
 S is the (P, U_p) state common to a stationary target and a flyer plate at the time of collision

REFERENCES

1. Napadensky, H. S., Development of Methods for Predicting the Response of Explosive Material to Impact (U), AFSWC TR 61-8, DASA 1225, March 1961 (SRD).
2. Napadensky, H. S., The Effects of Impact Loading on Plastic-Bonded Explosive Materials, DASA 1391, April 1963.
3. Napadensky, H. S., The Impact Vulnerability of the MLU-10/B Aerial Land Mine, ATL-TDR-64-60, January 1964, AD 447 917.
4. Kennedy, J. E., and H. S. Napadensky, The Vulnerability of Special Weapons to Fire and Impact (U), DASA 1276, Vol. V, Part 2, January 1964, (SRD).
5. Hornig, D. C., "Standardization of High Explosive Sensitiveness Tests," International Conference on Sensitivity and Hazards of Explosives, London, October 1963.
6. Weber, J. P., Factors Affecting the Vulnerability of Atomic Weapons to Impact, AFSWP Report No. 1132, January 1959. (S)
7. Jaffe, I., R. Beauregard, and A. Amster, "Determination of the Shock Pressure Required to Initiate Detonation of an Acceptor in the Shock Sensitivity Test," ARS J. 32, 22-25, 1962.
8. Hubbard, H. W., and M. H. Johnson, "Initiation of Detonations," J. Appl. Phys. Vol. 30, No. 5, May 1959.
9. Napadensky, H. S., The Impact Vulnerability of the Tritonal-Loaded MLU-10/B Aerial Land Mine, IITRI Report No. T6053-FR for AFSC under Contract No. AF 08(635)-3789, April 1965.
10. Napadensky, H. S., "Initiation of Explosives by Low Velocity Impact," The Fourth Symposium on Detonation, p. C-161, October 1965.
11. Liddiard, T. P., Jr., "The Initiation of Burning in High Explosives by Shock Waves," The Fourth Symposium on Detonation, p. C-109, October 1965.
12. Bowden, F. P., "The Initiation and Growth of Explosion in the Condensed Phase," Ninth International Symposium on Combustion, p. 499, Academic Press, New York, 1963.
13. Bowden, F. P., and A. D. Yoffe, Initiation and Growth of Explosions in Liquid and Solids, University Press, Cambridge, 1952.

REFERENCES (Cont.)

14. Bowden, F. P., "Introduction," Proceedings of the Royal Society, Series A Mathematical and Physical Sciences, No. 1245, Vol. 246, July 1958.
15. Weston, A. M., "Code Crash," A Study of the Impact Ignition of a Thin Wafer of Explosive Material, Document No. 4500-95-3-R28, Lawrence Radiation Laboratory, Livermore, California, March 1966.
16. James, Ed., Lawrence Radiation Laboratory, Livermore, California, Private Communication, Jan. 13, 1965.
17. Nadai, A., Theory of Flow and Fracture of Solids, McGraw-Hill Book Co., Inc., New York, 1963.
18. Bird, R. B., W. E. Stewart, and E. N. Lightfoot, Transport Phenomena, John Wiley & Sons, Inc., New York, 1960.
19. Liddiard, T. P., Jr., and S. J. Jacobs, Initiation of Reaction in Explosives by Shocks, NOLTR 64-53, October 1965.
20. Aronica, L., Sound Velocity and Elastic Moduli Measurements on Several TNT-Base Explosive Compositions, (U), NAVORD Report No. 6087, February 1961.
21. Gittings, E. F., "Initiation of a Solid Explosive by a Short Duration Shock" The Fourth Symposium on Detonation, p. C-15, October 1965.
22. Marlow, W. R., "Detonation Caused by the Reflection of Divergent Waves," The Fourth Symposium on Detonation, p. C-90, October 1965.
23. Hill, R., The Mathematical Theory of Plasticity, Oxford University Press, London, 1950, pp. 213-220, NWL Report No. 1914, NAVWEPS Report No. 8337.
24. Soper, W. G., "Wedge Penetration in a Thick Target," NWL Report No. 1914, NAVWEPS Report No. 8337, BUWEPS Task Assignment No. R01101001, May 1964.
25. Nanmac Thermocouples, Bulletin No. TB160, Nanmac Corporation, Needham Hts., Mass.
26. Eichler, J. B., "Computational Procedure for Stress-Wave Propagation in Elastic-Plastic Compactible Media, FR," IITRI-578 P21-10, Contract AT(11-1)-578 for USAEC, 1966.

DOCUMENT CONTROL DATA - R&D		
(Security classification of title, body of abstract and indexing annotation must be entered when the overall report is classified)		
1. ORIGINATING ACTIVITY (Corporate author) IIT Research Institute 10 West 35th Street Chicago, Illinois 60616		2a. REPORT SECURITY CLASSIFICATION U
		2b. GROUP ---
3. REPORT TITLE BEHAVIOR OF EXPLOSIVE SYSTEMS UNDER MILD IMPACT		
4. DESCRIPTIVE NOTES (Type of report and inclusive dates) Final Report, Ncv 1964 to Apr 1966		
5. AUTHOR(S) (Last name, first name, initial) Napacensky, H. S., and Kennedy, J. E.		
6. REPORT DATE May 1966	7a. TOTAL NO. OF PAGES 81	7b. NO. OF REFS 26
8a. CONTRACT OR GRANT NO. DA-49-146-XZ-374	8b. ORIGINATOR'S REPORT NUMBER(S) DASA - 1801	
9. PROJECT NO. T6111	9a. OTHER REPORT NO(S) (Any other numbers that may be assigned this report) T6111 - FR	
10. AVAILABILITY/LIMITATION NOTICES Each transmittal of this document outside the agencies of the U. S. Government must have prior approval of the Director, Defense Atomic Support Agency, Washington, D.C.		
11. SUPPLEMENTARY NOTES	12. SPONSORING MILITARY ACTIVITY Defense Atomic Support Agency	
13. ABSTRACT Analytical and experimental studies were carried out to increase the understanding of the behavior of high explosives under impact loads. A mathematical model was constructed assuming that a single mechanism, viscous heating, was operating during the radial extrusion of a flat explosive billet. To check the adequacy of the analytical model, the temperature profile at the explosive-anvil interface was continuously monitored using rapid response (1-5 μ sec) surface thermocouples. To extend the applicability of the IITRI-developed method for predicting impact velocities required for the initiation of the explosive components of special weapons, basic sensitivity data was acquired for 9010 PBX, Comp B-3 and 9404 PBX. The explosives were subjected to a concentrated impact load by means of a wedge-shaped loading device and to planar uniform loads having loads having two different pulse shapes.		
14. KEY WORDS Explosives Sensitivity Detonation Shock waves Initiation		



Defense Threat Reduction Agency

45045 Aviation Drive
Dulles, VA 20166-7517

CPWC/TRC

November 3, 1999

MEMORANDUM FOR DEFENSE TECHNICAL INFORMATION CENTER
ATTN: OCQ/MR WILLIAM BUSH

SUBJECT: DOCUMENT CHANGES

The Defense Threat Reduction Agency Security Office
has performed a classification/distribution statement
review for the following documents:

DASA-2519-1, AD-873313, STATEMENT A -
DASA-2536, AD-876697, STATEMENT A -
DASA-2519-2, AD-874891, STATEMENT A -
DASA-2156, AD-844800, STATEMENT A -
DASA-2083, AD-834874, STATEMENT A -
-DASA-1801, AD-487455, STATEMENT A -
POR-4067, AD-488079, STATEMENT C, -
ADMINISTRATIVE/OPERATIONAL USE
DASA-2228-1, AD-851256, STATEMENT C, *no target*
ADMINISTRATIVE/OPERATIONAL USE *only chg'd from SA to admin/op use.*
RAND-RM-2076, AD-150693, STATEMENT D, -
ADMINISTRATIVE/OPERATIONAL USE
7* AD-089546, STATEMENT A, ADMINISTRATIVE/OPERATIONAL USE * *ST-A*
DASA-1847, AD-379061, UNCLASSIFIED, STATEMENT C, - *JUN '65*
ADMINISTRATIVE/OPERATIONAL USE *NOT IN DTC*
RAND-RM-4812-PR, ELEMENTS OF A FUTURE BALLISTIC *370168*
MISSILE TEST PROGRAM, UNCLASSIFIED, STATEMENT C, *cert*
ADMINISTRATIVE/OPERATIONAL USE *Authority to Declassify*

If you have any questions, please call me at 703-325-1034.

Arndith Jarrett

ARDITH JARRETT
Chief, Technical Resource Center

*Leave ST-A
Per A. Jarrett
23 Nov 99*